The protonmotive force and respiratory control:

Building blocks of mitochondrial physiology

Part 1.

MitoEAGLE Network

Corresponding author: Gnaiger E

Contributing co-authors

Ahn B, Alves MG, Amati F, Åsander Frostner E, Bailey DM, Bastos Sant'Anna Silva AC, Battino M, Beard DA, Ben-Shachar D, Bishop D, Breton S, Brown GC, Brown RA, Buettner GR, Carvalho E, Cervinkova Z, Chang SC, Chicco AJ, Coen PM, Collins JL, Crisóstomo L, Davis MS, Dias T, Distefano G, Doerrier C, Ehinger J, Elmer E, Fell DA, Ferko M, Ferreira JCB, Filipovska A, Fisar Z, Fisher J, Garcia-Roves PM, Garcia-Souza LF, Genova ML, Gonzalo H, Goodpaster BH, Gorr TA, Han J, Harrison DK, Hellgren KT, Hernansanz P, Holland O, Hoppel CL, Iglesias-Gonzalez J, Irving BA, Iyer S, Jackson CB, Jansen-Dürr P, Jespersen NR, Jha RK, Kaambre T, Kane DA, Kappler L, Keijer J, Komlodi T, Kopitar-Jerala N, Krako Jakovljevic N, Kuang J, Labieniec-Watala M, Lai N, Laner V, Lee HK, Lemieux H, Lerfall J, Lucchinetti E, MacMillan-Crow LA, Makrecka-Kuka M, Meszaros AT, Moisoi N, Molina AJA, Montaigne D, Moore AL, Murray AJ, Newsom S, Nozickova K, O'Gorman D, Oliveira PF, Oliveira PJ, Orynbayeva Z, Pak YK, Palmeira CM, Patel HH, Pesta D, Petit PX, Pichaud N, Pirkmajer S, Porter RK, Pranger F, Prochownik EV, Radenkovic F, Reboredo P, Renner-Sattler K, Robinson MM, Rohlena J, Røsland GV, Rossiter HB, Salvadego D, Scatena R, Schartner M, Scheibye-Knudsen M, Schilling JM, Schlattner U, Schoenfeld P, Scott GR, Singer D, Sobotka O, Spinazzi M, Stier A, Stocker R, Sumbalova Z, Suravajhala P, Tanaka

27   M, Tandler B, Tepp K, Tomar D, Towheed A, Trivigno C, Tronstad KJ, Trougakos IP,

28   Tyrrell DJ, Velika B, Vendelin M, Vercesi AE, Victor VM, Wagner BA, Ward ML, Watala

29   C, Wei YH, Wieckowski MR, Wohlwend M, Wolff J, Wuest RCI, Zaugg K, Zaugg M,

30   Zorzano A

31

32   Supporting co-authors:

33   Arandarčikaitė O, Bakker BM, Bernardi P, Boetker HE, Borsheim E, Borutaitė V, Bouitbir J,

34   Calabria E, Calbet JA, Chaurasia B, Clementi E, Coker RH, Collin A, Das AM, De Palma C,

35   Dubouchaud H, Duchen MR, Durham WJ, Dyrstad SE, Engin AB, Fornaro M, Gan Z, Garlid

36   KD, Garten A, Gourlay CW, Granata C, Haas CB, Haavik J, Haendeler J, Hand SC, Hepple

37   RT, Hickey AJ, Hoel F, Kainulainen H, Keppner G, Khamoui AV, Klingenspor M, Koopman

38   WJH, Kowaltowski AJ, Krajcova A, Lenaz G, Malik A, Markova M, Mazat JP, Menze MA,

39   Methner A, Muntané J, Muntean DM, Neuzil J, Oliveira MT, Pallotta ML, Parajuli N,

40   Pettersen IKN, Porter C, Pulinilkunnil T, Ropelle ER, Salin K, Sandi C, Sazanov LA,

41   Siewiera K, Silber AM, Skolik R, Smenes BT, Soares FAA, Sokolova I, Sonkar VK,

42   Stankova P, Swerdlow RH, Szabo I, Trifunovic A, Thyfault JP, Tretter L, Vieyra A, Votion

43   DM, Williams C

44

45   **Updates:**

46   http://www.mitoeagle.org/index.php/MitoEAGLE_preprint_2017-09-21

47

Correspondence: Gnaiger E

Department of Visceral, Transplant and Thoracic Surgery, D. Swarovski Research Laboratory, Medical University of Innsbruck, Innrain 66/4, A-6020 Innsbruck, Austria
Email: erich.gnaiger@i-med.ac.at
Tel: +43 512 566796, Fax: +43 512 566796 20

This manuscript on 'The protonmotive force and respiratory control' is a position statement in the frame of COST Action CA15203 MitoEAGLE. The list of co-authors evolved from MitoEAGLE Working Group Meetings and a **bottom-up** *spirit of COST in phase 1: This is an open invitation to scientists and students to join as co-authors, to provide a balanced view on mitochondrial respiratory control, a fundamental introductory presentation of the concept of the protonmotive force, and a consensus statement on reporting data of mitochondrial respiration in terms of metabolic flows and fluxes. We plan a series of follow-up reports by the expanding MitoEAGLE Network, to increase the scope of recommendations on harmonization and facilitate global communication and collaboration.*
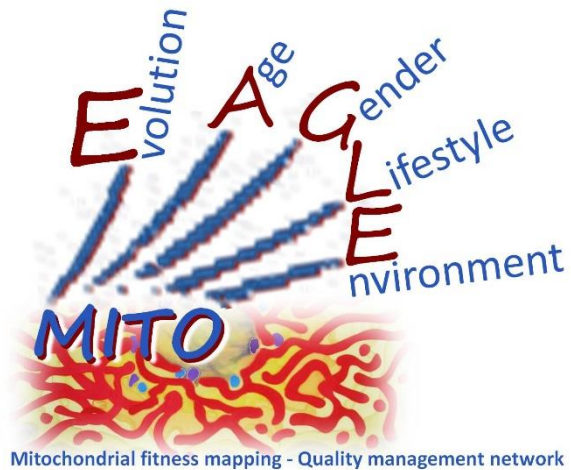
Phase 2: MitoEAGLE preprint (Versions 01 – 10): We continue to invite comments and suggestions on the, particularly if you are an **early career investigator adding an open future-oriented perspective**, *or an* **established scientist providing a balanced historical basis**. *Your critical input into the quality of the manuscript will be most welcome, improving our aims to be educational, general, consensus-oriented, and practically helpful for students working in mitochondrial respiratory physiology.*

Phase 3 (2017-11-11 or after MiP2017 and MitoEAGLE workshop in Hradec Kralove): **Manuscript submission to a preprint server, such as BioRxiv. We want to invite further opinion leaders:** *To join as a co-author, please feel free to focus on a particular section in terms of direct input and references, contributing to the scope of the manuscript from the perspective of your expertise. Your comments will be largely posted on the discussion page of the MitoEAGLE preprint website.*

If you prefer to submit comments in the format of a referee's evaluation rather than a contribution as a co-author, I will be glad to distribute your views to the updated list of co-authors for a balanced response. We would ask for your consent on this open bottom-up policy.

Phase 4: We organize a MitoEAGLE session linked to our series of reports at the MiPconference Nov 2017 in Hradec Kralove in close association with the MiPsociety (where you hopefully will attend) and at EBEC 2018 in Budapest.

» http://www.mitoeagle.org/index.php/MiP2017_Hradec_Kralove_CZ

I thank you in advance for your feedback.
With best wishes,

Erich Gnaiger
Chair Mitochondrial Physiology Society - http://www.mitophysiology.org
Chair COST Action MitoEAGLE - http://www.mitoeagle.org
Medical University of Innsbruck, Austria

Contents

146 **Abstract**

147 Clarity of concept and consistency of nomenclature are key trademarks of a research field.

148 These trademarks facilitate effective transdisciplinary communication, education, and

149 ultimately further discovery. As the knowledge base and importance of mitochondrial

150 physiology to human health expand, the necessity for harmonizing nomenclature concerning

151 mitochondrial respiratory states and rates has become increasingly apparent. Peter Mitchell's

152 concept of the protonmotive force establishes the links between electrical and chemical

153 components of energy transformation and coupling in oxidative phosphorylation. This unifying

154 concept provides the framework for developing a consistent nomenclature for mitochondrial

155 physiology and bioenergetics. Herein, we follow IUPAC guidelines on general terms of

156 physical chemistry, extended by the concepts of open systems and irreversible thermodynamics.

157 We align the nomenclature of classical bioenergetics on respiratory states with a concept-driven

158 constructive terminology to address the meaning of each respiratory state. Furthermore, we

159 suggest uniform standards for the evaluation of respiratory states that will ultimately support

160 the development of databases of mitochondrial respiratory function in species, tissues and cells

161 studied under diverse physiological and experimental conditions. In this position statement, in

162 the frame of COST Action CA15203 MitoEAGLE, we endeavour to provide a balanced view

163 on mitochondrial respiratory control, a fundamental introductory presentation of the concept of

164 the protonmotive force, and a critical discussion on reporting data of mitochondrial respiration

165 in terms of metabolic flows and fluxes.

166

167 *Keywords:* Mitochondrial respiratory control, coupling control, mitochondrial

168 preparations, protonmotive force, chemiosmotic theory, oxidative phosphorylation, OXPHOS,

169 efficiency, electron transfer, ET; proton leak, LEAK, residual oxygen consumption, ROX, State

170 2, State 3, State 4, normalization, flow, flux

171

172

Box 1:

In brief:
mitochondria
and Bioblasts

> * Does the public expect biologists to understand Darwin's theory of evolution?
> * Do students expect that researchers of bioenergetics can explain Mitchell's theory of chemiosmotic energy transformation?

Mitochondria were described for the first time in 1857 by Rudolph Albert Kölliker as granular structures or 'sarkosomes' *(a reference is needed)*. In 1886 *(a reference is needed)* Richard Altmann called them 'bioblasts' (published 1894). The word 'mitochondrium' (Greek mitos: thread; chondros: granule) was introduced by Carl Benda (1898). Mitochondria are the oxygen-consuming electrochemical generators which evolved from endosymbiotic bacteria (Margulis 1970; Lane 2005). The bioblasts of Richard Altmann (1894) included not only the mitochondria as presently defined, but also symbiotic and free-living bacteria.

We now recognize mitochondria as dynamic organelles with a double membrane that are contained within eukaryotic cells. The mitochondrial inner membrane (mtIM) shows dynamic tubular to disk-shaped cristae that separate the mitochondrial matrix, *i.e.* the internal mitochondrial compartment, and the intermembrane space; the latter being enclosed by the mitochondrial outer membrane (mtOM). Mitochondria are the structural and functional elemental units of cell respiration. Cell respiration is the consumption of oxygen by electron transfer coupled to electrochemical proton translocation across the mtIM. In the process of oxidative phosphorylation (OXPHOS), the reduction of O_2 is electrochemically coupled to the transformation of energy in the form of adenosine triphosphate (ATP; Mitchell 1961, 2011). These powerhouses of the cell contain the machinery of the OXPHOS-pathway, including transmembrane respiratory complexes (*i.e.* proton pumps with FMN, Fe-S and cytochrome *b*, *c*, aa_3 redox systems); alternative dehydrogenases and oxidases; the coenzyme ubiquinone (Q); ATP synthase; the enzymes of the tricarboxylic acid cycle and the fatty acid oxidation enzymes; transporters of ions, metabolites and co-factors; and mitochondrial kinases related to energy transfer pathways. The mitochondrial proteome comprises over 1,200 proteins

200   (MITOCARTA), mostly encoded by nuclear DNA (nDNA), with a variety of functions, many

201   of which are relatively well known (*e.g.* apoptosis-regulating proteins), while others are still

202   under investigation, or need to be identified (*e.g.* alanine transporter).

203   Mitochondria typically maintain several copies of their own genome (hundred to

204   thousands per cell; Cummins 1998), which is almost exclusively maternally inherited (White *et*

205   *al.* 2008) and known as mitochondrial DNA (mtDNA). One exception to strictly maternal

206   inheritance in animals is found in bivalves (Breton *et al.* 2007). mtDNA is 16.5 Kb in length,

207   contains 13 protein-coding genes for subunits of the transmembrane respiratory Complexes CI,

208   CIII, CIV and ATP synthase, and also encodes 22 tRNAs and the mitochondrial 16S and 12S

209   rRNA. The mitochondrial genome is both regulated and supplemented by nuclear-encoded

210   mitochondrial targeted proteins. Evidence has accumulated that additional gene content is

211   encoded in the mitochondrial genome, *e.g.* microRNAs, piRNA, smithRNAs, repeat associated

212   RNA, and even additional proteins (Duarte *et al.* 2014; Lee *et al.* 2015; Cobb *et al.* 2016).

213   The mtIM contains the non-bilayer phospholipid cardiolipin, which is not present in any

214   other eukaryotic cellular membrane. Cardiolipin promotes the formation of respiratory

215   supercomplexes, which are supramolecular assemblies based upon specific, though dynamic,

216   interactions between individual respiratory complexes (Greggio *et al.* 2017; Lenaz *et al.* 2017).

217   Membrane fluidity is an important parameter influencing functional properties of proteins

218   incorporated in the membranes (Waczulikova *et al.* 2007). There is a constant crosstalk between

219   mitochondria and the other cellular components, maintaining cellular mitostasis through

220   regulation at both the transcriptional and post-translational level, and through cell signalling

221   including proteostatic (e.g. the ubiquitin-proteasome and autophagy-lysosome pathways) and

222   genome stability modules thoughout the cell cycle or even cell death, contributing to

223   homeostatic regulation in response to varying energy demands and stress (Quiros *et al.* 2016).

224   In addition to mitochondrial movement along the microtubules, mitochondrial morphology can

225   change in response to the energy requirements of the cell via processes known as fusion and

fission, through which mitochondria can communicate within a network, and in response to intracellular stress factors causing swelling and ultimately permeability transition.

Mitochondrial dysfunction is associated with a wide variety of genetic and degenerative diseases. Robust mitochondrial function is supported by physical exercise and caloric balance, and is central for sustained metabolic health throughout life. Therefore, a better understanding of mitochondrial physiology will improve our understanding of the etiology of disease, the diagnostic repertoire of mitochondrial medicine, with a focus on protective medicine, lifestyle and healthy aging.

Abbreviation: mt, as generally used in mtDNA. Mitochondrion is singular and mitochondria is plural.

'*For the physiologist, mitochondria afforded the first opportunity for an experimental approach to structure-function relationships, in particular those involved in active transport, vectorial metabolism, and metabolic control mechanisms on a subcellular level*' (Ernster and Schatz 1981).

---

1. Introduction

Mitochondria are the powerhouses of the cell with numerous physiological, molecular, and genetic functions (**Box 1**). Every study of mitochondrial function and disease is faced with **E**volution, **A**ge, **G**ender and sex, **L**ifestyle, and **E**nvironment (EAGLE) as essential background conditions intrinsic to the individual patient or subject, cohort, species, tissue and to some extent even cell line. As a large and highly coordinated group of laboratories and researchers, the mission of the global MitoEAGLE Network is to generate the necessary scale, type, and quality of consistent data sets and conditions to address this intrinsic complexity. Harmonization of experimental protocols and implementation of a quality control and data management system is required to interrelate results gathered across a spectrum of studies and to generate a rigorously monitored database focused on mitochondrial respiratory function. In this way,

252 researchers within the same and across different disciplines will be positioned to compare their

253 findings to an agreed upon set of clearly defined and accepted international standards.

254   Reliability and comparability of quantitative results depend on the accuracy of

255 measurements under strictly-defined conditions. A conceptually defined framework is also

256 required to warrant meaningful interpretation and comparability of experimental outcomes

257 carried out by research groups at different institutes. With an emphasis on quality of research,

258 collected data can be useful far beyond the specific question of a particular experiment.

259 Enabling meta-analytic studies is the most economic way of providing robust answers to

260 biological questions (Cooper *et al.* 2009). Vague or ambiguous jargon can lead to confusion

261 and may relegate valuable signals to wasteful noise. For this reason, measured values must be

262 expressed in standardized units for each parameter used to define mitochondrial respiratory

263 function. Standardization of nomenclature and definition of technical terms is essential to

264 improve the awareness of the intricate meaning of a divergent scientific vocabulary, for

265 documentation and integration into databases in general, and quantitative modelling in

266 particular (Beard 2005). The focus on the protonmotive force, coupling states, and fluxes

267 through metabolic pathways of aerobic energy transformation in mitochondrial preparations is

268 a first step in the attempt to generate a harmonized and conceptually-oriented nomenclature in

269 bioenergetics and mitochondrial physiology. Coupling states of intact cells and respiratory

270 control by fuel substrates and specific inhibitors of respiratory enzymes will be reviewed in

271 subsequent communications.

272

273 **2. Respiratory coupling states in mitochondrial preparations**

274   '*Every professional group develops its own technical jargon for talking about*

275   *matters of critical concern ... People who know a word can share that idea with*

276   *other members of their group, and a shared vocabulary is part of the glue that holds*

277   *people together and allows them to create a shared culture*' (Miller 1991).

278   **Mitochondrial preparations** are defined as either isolated mitochondria, or tissue and

279   cellular preparations in which the barrier function of the plasma membrane is disrupted. The

280   plasma membrane separates the cytosol, nucleus, and organelles (the intracellular

281   compartment) from the environment of the cell. The plasma membrane consists of a lipid

282   bilayer, embedded proteins, and attached organic molecules that collectively control the

283   selective permeability of ions, organic molecules, and particles across the cell boundary. The

284   intact plasma membrane, therefore, prevents the passage of many water-soluble mitochondrial

285   substrates, such as succinate or adenosine diphosphate (ADP), that are required for the analysis

286   of respiratory capacity at kinetically-saturating concentrations, thus limiting the scope of

287   investigations into mitochondrial respiratory function in intact cells. The cholesterol content of

288   the plasma membrane is high compared to mitochondrial membranes. Therefore, mild

289   detergents, such as digitonin and saponin, can be applied to selectively permeabilize the plasma

290   membrane by interaction with cholesterol and allow free exchange of cytosolic components

291   with ions and organic molecules of the immediate cell environment, while maintaining the

292   integrity and localization of organelles, cytoskeleton, and the nucleus. Application of optimum

293   concentrations of these mild detergents leads to the complete loss of cell viability, tested by

294   nuclear staining, while mitochondrial function remains intact, as shown by an unaltered

295   respiration rate of isolated mitochondria after the addition of such low concertations of digitonin

296   and saponin. In addition to mechanical permeabilization during homogenization of fresh tissue,

297   saponin may be applied to ensure permeabilization of all cells. Crude homogenate and cells

298   permeabilized in the respiration chamber contain all components of the cell at highly diluted

299   concentrations. All mitochondria are retained in chemically-permeabilized mitochondrial

300   preparations and crude tissue homogenates. In the preparation of isolated mitochondria, the

301   cells or tissues are homogenized, and the mitochondria are separated from other cell fractions

302   and purified by differential centrifugation, entailing the loss of a significant fraction of

303   mitochondria. The term mitochondrial preparation does not include further fractionation of

304   mitochondrial components, as well as submitochondrial particles.

305

306   *2.1. Three coupling states of mitochondrial preparations and residual oxygen consumption*

307   **Respiratory capacities in coupling control states:** To extend the classical nomenclature

308   on mitochondrial coupling states (Section 2.4) by a concept-driven terminology that

309   incorporates explicit information on the nature of the respiratory states, the terminology must

310   be general and not restricted to any particular experimental protocol or mitochondrial

311   preparation (Gnaiger 2009). We focus primarily on the conceptual 'why', along with

312   clarification of the experimental 'how'. In the following section, the concept-driven

313   terminology is explained and coupling states are defined. We define respiratory capacities,

314   comparable to channel capacity in information theory (Schneider 2006), as the upper bound of

315   the rate of respiration measured in defined coupling and electron transfer-pathway (ET-

316   pathway) control states. To provide a diagnostic reference for respiratory capacities of core

317   energy metabolism, the capacity of *oxidative phosphorylation*, OXPHOS, is measured at

318   kinetically-saturating concentrations of ADP and inorganic phosphate, P_i. The *oxidative* ET-

319   capacity reveals the limitation of OXPHOS-capacity mediated by the *phosphorylation-*

320   pathway. The ET- and phosphorylation-pathways comprise coupled segments of the OXPHOS-

321   pathway. ET-capacity is measured as noncoupled respiration by application of *external*

322   *uncouplers*. The contribution of *intrinsically uncoupled* oxygen consumption is most easily

323   studied in the absence of ADP, *i.e.* by not stimulating phosphorylation, or by inhibition of the

324   phosphorylation-pathway. The corresponding states are collectively classified as LEAK-states,

325   when oxygen consumption compensates mainly for the proton leak (**Table 1**). Different

326   coupling states are induced by: (*1*) adding ADP or P_i; (*2*) inhibiting the phosphorylation-

327   pathway; and (*3*) performing uncoupler titrations, while maintaining a defined ET-pathway

328   state with constant fuel substrates and ET inhibitors (**Fig. 1**).

329   **Kinetic control:** Coupling control states are established in the study of mitochondrial

330   preparations to obtain reference values for various output variables. Physiological conditions *in*

331   *vivo* deviate from these experimentally obtained states. Since kinetically-saturating

332   concentrations, *e.g.* of ADP or oxygen, may not apply to physiological intracellular conditions,

333   relevant information is obtained in studies of kinetic responses to conditions intermediate

334   between the LEAK state at zero [ADP] and the OXPHOS-state at saturating [ADP], or of

335   respiratory capacities in the range between kinetically-saturating [O_2] and anoxia (Gnaiger

336   2001).

337   **Specification of dose of biochemical additions:** Nominal concentrations of substrates,

338   uncouplers, inhibitors, and other biochemical reagents titrated to dissect mitochondrial function

339   are usually reported as initial amount of substance concentration [$mol \cdot L^{-1}$] in the incubation

340   medium. When aiming at the measurement of kinetically saturated processes such as OXPHOS

341   capacities, the concentrations for substrates can be chosen in light of the K_m'. In the case of

342   hyperbolic kinetics, only 80% of maximum respiratory capacity is obtained at a substrate

343   concentration of four times the K_m', whereas substrate concentrations of 9, 19 and 49 times the

344   K_m' are theoretically required for reaching 90%, 95% or 98% of the maximal rate. Other

345   reagents are chosen to inhibit or alter some process. The amount of these tools in an

346   experimental incubation is selected to maximize effect, yet not lead to unacceptable off-target

347   consequences that would adversely affect the data being sought. Specifying the amount of

348   substance in an incubation as nominal concentration in the aqueous incubation medium can be

349   ambiguous (Doskey *et al*. 2015), particularly when lipid-soluble substances (oligomycin;

350   uncouplers) or cations (TPP+; fluorescent dyes such as safranin, TMRM) are applied which

351   accumulate in biological membranes or in the mitochondrial matrix, respectively. For example,

352   a dose of digitonin of 8 fmol·cell^{-1} (10 µg·10^{-6} cells) is optimal for permeabilization of

353   endothelial cells, and the concentration in the incubation medium has to be adjusted according

354   to the cell density applied (Pesta and Gnaiger 2012). Generally, dose/exposure can be specified

per unit of biological sample, *i.e.* (nominal moles of xenobiotic)/(number of cells) [mol·cell^{-1}]
or, as appropriate, per mass of biological sample [mol·g^{-1}]. This approach to specification of
dose/exposure provides a scalable parameter that can be used to design experiments, help
interpret a wide variety of experimental results, and provide absolute information that allows
researchers worldwide to make the most use of published data (Doskey *et al.* 2015).
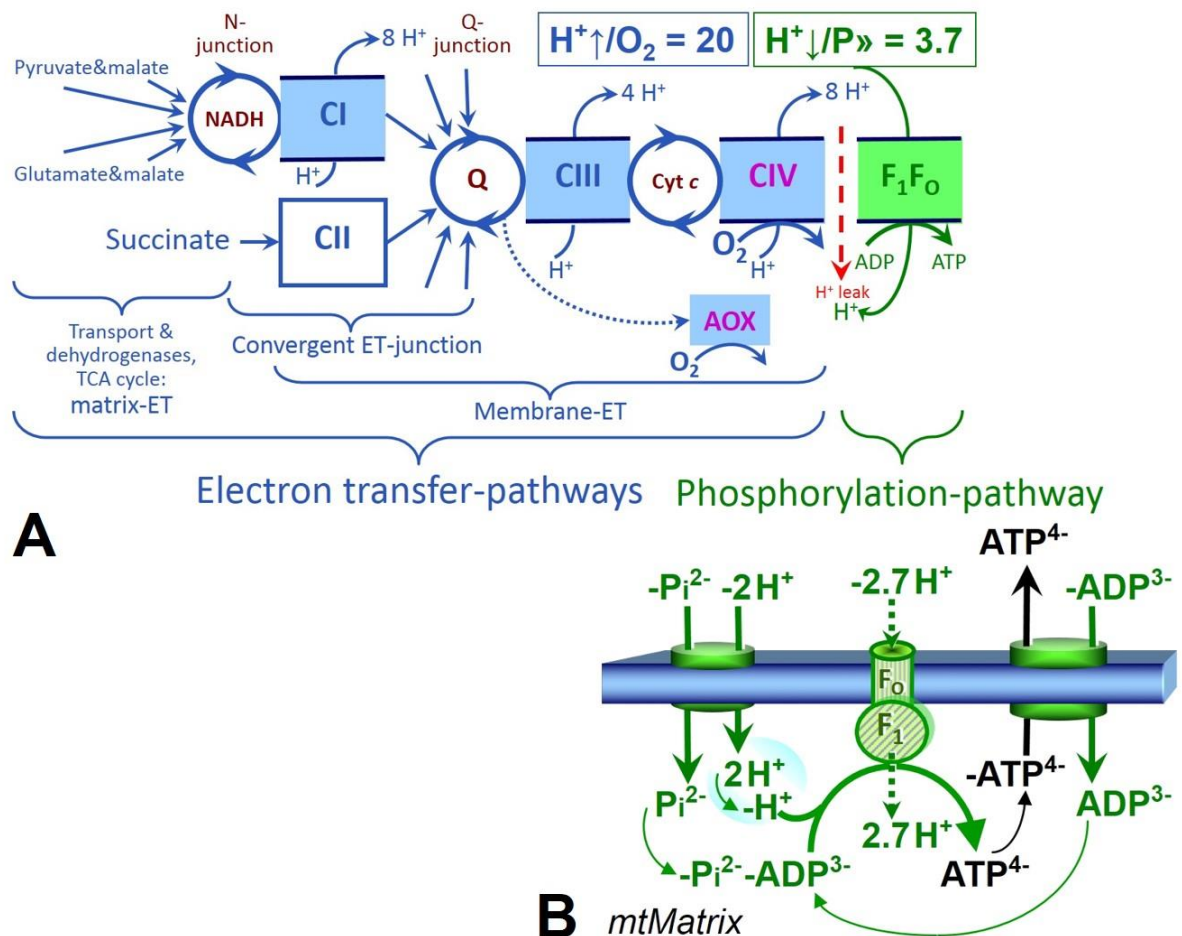
Fig. 1. The oxidative phosphorylation-pathway, OXPHOS-pathway. (A) Electron transfer,
ET, coupled to phosphorylation. ET-pathways converge at the N- and Q-junction, as shown for
the NADH- and succinate-pathway; additional arrows indicate electron entry to the Q-junction
through electron transferring flavoprotein, glycerophosphate dehydrogenase, dihydro-orotate
dehydrogenase, choline dehydrogenase, and sulfide-ubiquinone oxidoreductase. The branched
pathway of oxygen consumption by alternative quinol oxidase (AOX) is indicated by the dotted

368   arrow. The $H^+\uparrow/O_2$ ratio is the outward proton flux from the matrix space divided by catabolic

369   O_2 flux in the NADH-pathway. The $H^+\downarrow/P»$ ratio is the inward proton flux from the inter-

370   membrane space divided by the flux of phosphorylation of ADP to ATP. Due to proton leak

371   and slip these are not fixed stoichiometries. (**B**) Phosphorylation-pathway catalyzed by the F_1F_O

372   ATP synthase, adenine nucleotide translocase, and inorganic phosphate transporter. The $H^+\downarrow/P»$

373   stoichiometry is the sum of the coupling stoichiometry in the ATP synthase reaction (-2.7 H^+

374   from the intermembrane space, 2.7 H^+ to the matrix) and the proton balance in the translocation

375   of ADP^{2-}, ATP^{3-} and P_i^{2-}. See Eqs. 3 and 4 for further explanation. Modified from (A) Lemieux

376   *et al*. (2017) and (B) Gnaiger (2014).

377
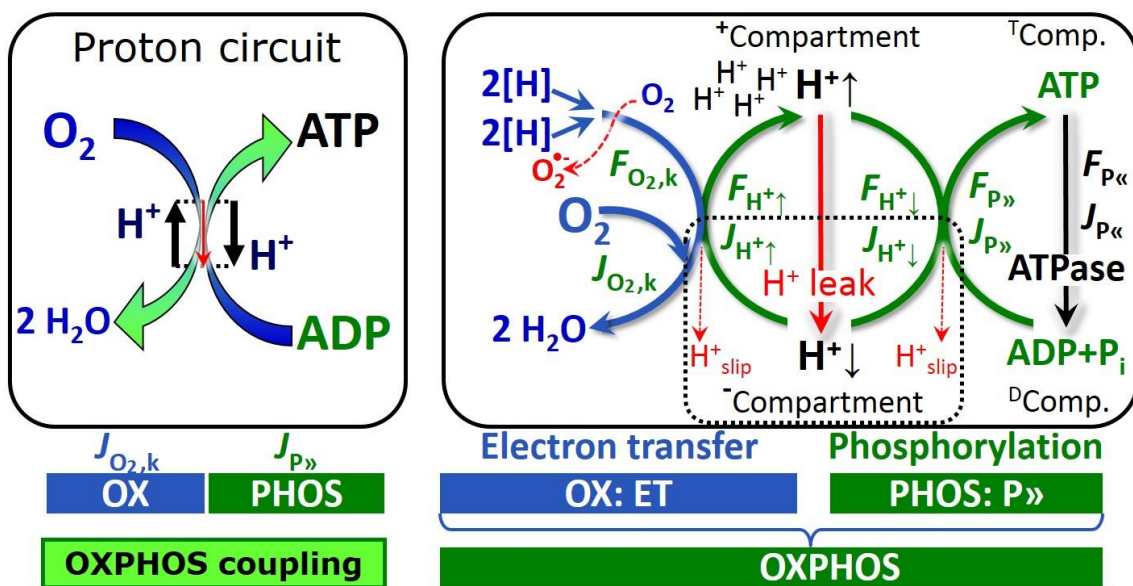
378

379   **Fig. 2. The proton circuit and coupling in oxidative phosphorylation (OXPHOS).** Oxygen

380   flux, $J_{O_2,k}$, through the catabolic ET-pathway k is coupled to flux through the phosphorylation-

381   pathway of ADP to ATP, $J_{P»}$, by the proton pumps of the ET-pathway, pushing the outward

382   proton flux, $J_{H^+\uparrow}$, and generating the output protonmotive force, $F_{H^+\uparrow}$. ATP synthase is coupled

383   to inward proton flux, $J_{H^+\downarrow}$, to phosphorylate ADP+P_i to ATP, driven by the input protonmotive

384   force, $F_{H^+\downarrow} = -F_{H^+\uparrow}$. 2[H] indicates the reduced hydrogen equivalents of fuel substrates that

385   provide the chemical input force, $F_{O_2,k}$ [kJ/mol O_2], of the catabolic reaction k with oxygen

386   (Gibbs energy of reaction per mole O_2 consumed in reaction k), typically in the range of -460

387   to -480 kJ/mol. The output force is given by the phosphorylation potential difference (ADP

388   phosphorylated to ATP), $F_{P»}$, which varies *in vivo* ranging from about 48 to 62 kJ/mol under

389   physiological conditions (Gnaiger 1993a). Fluxes, J_B, and forces, F_B, are expressed in either

390   chemical units, $[mol·s^{-1}·m^{-3}]$ and $[J·mol^{-1}]$ respectively, or electrical units, $[C·s^{-1}·m^{-3}]$ and $[J·C^{-1}]$

391   respectively. Vectorial and scalar fluxes are expressed per volume, V $[m^3]$, of the system. The

392   system defined by the boundaries shown as a full black line is not a black box, but is analysed

393   as a compartmental system. The negative compartment (˙Compartment, enclosed by the dotted

394   line) is the matrix space, separated from the positive compartment (⁺Compartment) by the

395   mtIM. ADP+P_i and ATP are the substrate- and product-compartments (scalar ADP and ATP

396   compartments, ^{D}Comp. and ^{T}Comp.), respectively. Chemical potentials of all substrates and

397   products involved in the scalar reactions are measured in the ⁺Compartment for calculation of

398   the scalar forces $F_{O_2,k}$ and $F_{P»} = -F_{P«}$ (**Box 2**). Modified from Gnaiger (2014).

399

400   **Phosphorylation, P»:** *Phosphorylation* in the context of OXPHOS is defined as

401   phosphorylation of ADP to ATP. On the other hand, the term phosphorylation is used generally

402   in many different contexts, *e.g.* protein phosphorylation. This justifies consideration of a

403   symbol more discriminating and specific than P as used in the P/O ratio (phosphate to atomic

404   oxygen ratio; O = 0.5 O_2), where P indicates phosphorylation of ADP to ATP or GDP to GTP.

405   We propose the symbol P» for the endergonic direction of phosphorylation ADP→ATP, and

406   likewise the symbol P« for the corresponding exergonic hydrolysis ATP→ADP (**Fig. 2; Box

407   3**). ATP synthase is the proton pump of the phosphorylation-pathway (**Fig. 1B**). P» may also

408   involve substrate-level phosphorylation as part of the tricarboxylic acid cycle (succinyl-CoA

409   ligase) and phosphorylation of ADP catalyzed by phosphoenolpyruvate carboxykinase,

410   adenylate kinase, creatine kinase, hexokinase and nucleoside diphosphate kinase (NDPK).

411   Kinase cycles are involved in intracellular energy transfer and signal transduction for regulation

412 of energy flux. In isolated mammalian mitochondria ATP production catalyzed by adenylate

413 kinase, 2ADP ↔ ATP + AMP, proceeds without fuel substrates in the presence of ADP

414 (Komlódi and Tretter 2017). $J_{P»}/J_{O_2,k}$ (P»/O$_2$) is two times the 'P/O' ratio of classical

415 bioenergetics. The effective P»/O$_2$ ratio is diminished by: (*1*) the proton leak across the mtIM

416 from low pH in the $^+$Compartment to high pH in the $^-$Compartment; (*2*) cycling of other cations;

417 (*3*) proton slip in the proton pumps when a proton effectively is not pumped; and (*4*) electron

418 leak in the univalent reduction of oxygen (O$_2$; dioxygen) to superoxide anion radical (O$_2^{•-}$).

419

420 **Table 1. Coupling states and residual oxygen consumption in mitochondrial**

421 **preparations in relation to respiration- and phosphorylation-rate, $J_{O_2,k}$ and $J_{P»}$,**

422 **and protonmotive force, $F_{H+↑}$.** Coupling states are established at kinetically-

423 saturating concentrations of fuel substrates and O$_2$.

State	$J_{O_2,k}$	$J_{P»}$	$F_{H+↑}$	Inducing factors	Limiting factors
LEAK	*L*; low proton leak-dependent respiration	0	max.	Proton leak, slip, and cation cycling	$J_{P»} = 0$: (*1*) without ADP, L_N; (*2*) max. ATP/ADP ratio, L_T; or (*3*) inhibition of the phosphorylation-pathway, L_{Omy}
OXPHOS	*P*; high ADP-stimulated respiration	max.	high	Kinetically-saturating [ADP] and [P$_i$]	$J_{P»}$ by phosphorylation-pathway; or $J_{O_2,k}$ by ET-capacity
ET	*E*; max. noncoupled respiration	0	low	Optimal external uncoupler concentration for max. oxygen flux	$J_{O_2,k}$ by ET-capacity
ROX	*Rox*; min. residual O$_2$ consumption	0	0	$J_{O_2,Rox}$ in non-ET-pathway oxidation reactions	Full inhibition of ET-pathway or absence of fuel substrates

424
425

426

427 **LEAK-state** (**Fig. 3**): The

428 LEAK-state is defined as a state

429 of mitochondrial respiration

430 when O_2 flux mainly

431 compensates for the proton leak

432 in the absence of ATP synthesis,

433 at kinetically-saturating

434 concentrations of O_2 and

435 respiratory fuel substrates.

436 LEAK-respiration is measured to
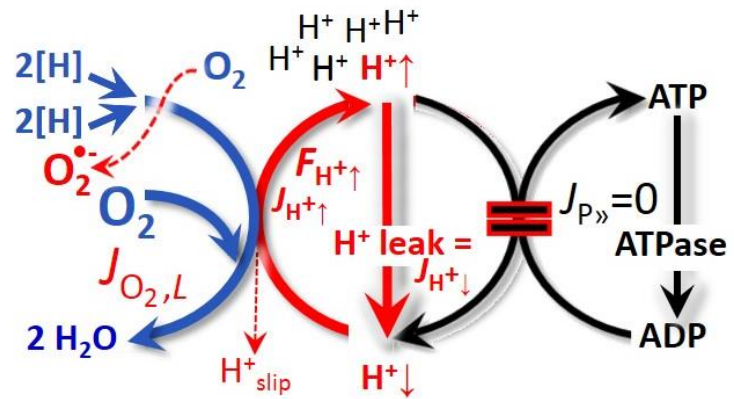
Fig. 3. LEAK-state: Phosphorylation is arrested, $J_{P»}$ = 0, and oxygen flux, $J_{O_2,L}$, is controlled mainly by the proton leak, which equals $J_{H^+\downarrow}$, at maximum protonmotive force, $F_{H^+\uparrow}$. See also Fig. 2.

437 obtain an indirect estimate of *intrinsic uncoupling* without addition of any experimental

438 uncoupler: (*1*) in the absence of adenylates; (*2*) after depletion of ADP at maximum ATP/ADP

439 ratio; or (*3*) after inhibition of the phosphorylation-pathway by inhibitors of ATP synthase, such

440 as oligomycin, or adenine nucleotide translocase, such as carboxyatractyloside. It is important

441 to consider adjustment of the nominal concentration of these inhibitors to the density of

442 biological sample applied, to minimize or avoid inhibitory side-effects exerted on ET-capacity

443 or even some uncoupling.

444 **Proton leak:** Proton leak is the *uncoupled* process in which protons diffuse across the

445 mtIM in the dissipative direction of the downhill protonmotive force without coupling to

446 phosphorylation (**Fig. 3**). The proton leak flux, $F_{H^+\downarrow}$, depends non-linearly on the protonmotive

447 force (Garlid *et al.* 1989; Divakaruni and Brand 2011), is a property of the mtIM, may be

448 enhanced due to possible contaminations by free fatty acids, and is physiologically controlled.

449 In particular, inducible uncoupling mediated by uncoupling protein 1 (UCP1) is physiologically

450 controlled, *e.g.*, in brown adipose tissue. UCP1 is a proton channel of the mtIM facilitating the

451 conductance of protons across the mtIM (Klingenberg 2017). As a consequence of this effective

short-circuit, the protonmotive force diminishes, resulting in stimulation of electron transfer to oxygen and heat dissipation without phosphorylation of ADP. Mitochondrial injuries may lead to *dyscoupling* as a pathological or toxicological cause of *uncoupled* respiration, *e.g.*, as a consequence of opening the permeability transition pore. Dyscoupled respiration is distinguished from the experimentally induced *noncoupled* respiration in the ET-state. Under physiological conditions, the proton leak is the dominant contributor to the overall leak current (Dufour *et al.* 1996).

Table 2. Distinction of terms related to coupling.

Term	Respiration	P»/O₂	Note
Fully coupled	$P - L$	max.	OXPHOS-capacity corrected for LEAK-respiration (**Fig. 6**)
Well-coupled	P	High	Phosphorylating respiration with an intrinsic LEAK component (**Fig. 4**)
Loosely coupled	up to E	Low	Inducibly uncoupled by UCP1 or Ca^{2+} cycling
Dyscoupled	P	Low	Pathologically, toxicologically, environmentally increased uncoupling, mitochondrial dysfunction
Uncoupled and Decoupled	L	0	Non-phosphorylating intrinsic LEAK-respiration without added protonophore (**Fig. 3**)
Noncoupled	E	0	Non-phosphorylating respiration stimulated to maximum flux at optimum exogenous uncoupler concentration (**Fig. 5**)

Proton slip: Proton slip is the *decoupled* process in which protons are only partially translocated by a proton pump of the ET-pathways and slip back to the original compartment (Dufour *et al.* 1996). Proton slip can also happen in association with the ATP-synthase, in which case the proton slips downhill across the membrane to the matrix without contributing to ATP synthesis. In each case, proton slip is a property of the proton pump and increases with the turnover rate of the pump.

468   **Cation cycling:** Proton leak is a leak current of protons. There can be other cation

469   contributors to leak current including calcium and probably magnesium. Calcium current is

470   balanced by mitochondrial Na/Ca exchange, which is balanced by Na/H exchange or K/H

471   exchange. This is another effective uncoupling mechanism different from proton leak and slip.
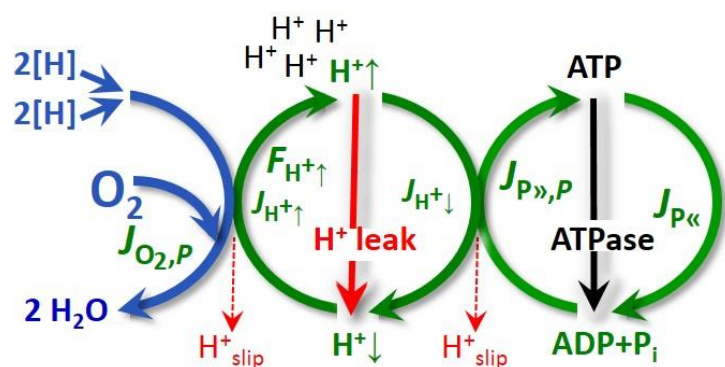
472   Small differences of terms, *e.g.*, uncoupled, noncoupled, are easily overlooked and may

473   be erroneously perceived as identical. Even with an attempt at rigorous definition, the common

474   use of such terms may remain vague (**Table 2**).

475   **OXPHOS-state** (**Fig. 4**):

476 The OXPHOS-state is defined as

477 the respiratory state with

478 kinetically-saturating

479 concentrations of O_2, respiratory

480 and phosphorylation substrates,

481 and absence of exogenous

482 uncoupler, which provides an

483 estimate of the maximal

484 respiratory capacity in the

485 OXPHOS-state for any given ET-

Fig. 4. OXPHOS-state: Phosphorylation, $J_{P»}$, is stimulated by kinetically-saturating [ADP] and inorganic phosphate, [P_i], and is supported by a high protonmotive force, $F_{H+↑}$. O_2 flux, $J_{O_2,P}$, is well-coupled at a P»/O_2 ratio of $J_{P»,P}/J_{O_2,P}$. See also Fig. 2.

486 pathway state. Respiratory capacities at kinetically-saturating substrate concentrations provide

487 reference values or upper limits of performance, aiming at the generation of data sets for

488 comparative purposes. Physiological activities and effects of substrate kinetics can be evaluated

489 relative to OXPHOS capacities.

490   As discussed previously, 0.2 mM ADP does not fully saturate flux in isolated

491 mitochondria (Gnaiger 2001; Puchowicz *et al.* 2004); greater ADP concentration is required,

492 particularly in permeabilized muscle fibres and cardiomyocytes, to overcome limitations by

493 intracellular diffusion and by the reduced conductance of the mitochondrial outer membrane,

494 mtOM (Jepihhina *et al.* 2011, Illaste *et al.* 2012, Simson *et al.* 2016), either through interaction

495 with tubulin (Rostovtseva *et al.* 2008) or other intracellular structures (Birkedal *et al.* 2014). In

496 permeabilized muscle fibre bundles of high respiratory capacity, the apparent K_m for ADP

497 increases up to 0.5 mM (Saks *et al.* 1998), indicating that >90% saturation is reached only at

498 >5 mM ADP. Similar ADP concentrations are also required for accurate determination of

499 OXPHOS-capacity in human clinical cancer samples and permeabilized cells (Klepinin *et al.*

500 2016; Koit *et al.* 2017). Whereas 2.5 to 5 mM ADP is sufficient to obtain the actual OXPHOS-

501 capacity in many types of permeabilized tissue and cell preparations, experimental validation

502 is required in each specific case.

503 **Electron transfer-state**

504 (**Fig. 5**): The ET-state is defined

505 as the *noncoupled* state with

506 kinetically-saturating

507 concentrations of O_2, respiratory

508 substrate and optimum

509 *exogenous* uncoupler

510 concentration for maximum O_2

511 flux, as an estimate of oxidative

512 ET-capacity. Inhibition of
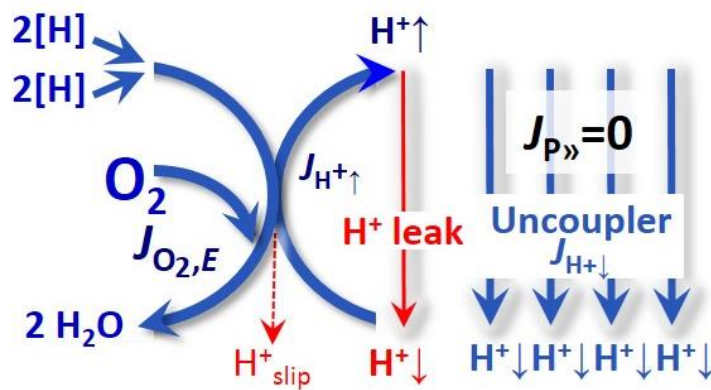
Fig. 5. ET-state: Noncoupled respiration, $J_{O2,E}$, is maximum at optimum exogenous uncoupler concentration and phosphorylation is zero, $J_{P»} = 0$ (See also Fig. 2).

513 respiration is observed at higher than optimum uncoupler concentrations. As a consequence of

514 the nearly collapsed protonmotive force, the driving force is insufficient for phosphorylation

515 and $J_{P»} = 0$.

516 Besides the three fundamental coupling states of mitochondrial preparations, the

517 following respiratory state also is relevant to assess respiratory function:

518 **ROX:** Residual oxygen consumption (ROX) is defined as O_2 consumption due to

519 oxidative side reactions remaining after inhibition of ET with rotenone, malonic acid and

520   antimycin A. Cyanide and azide not only inhibit CIV but several peroxidases which should be

521   involved in ROX. ROX is not a coupling state but represents a baseline that is used to correct

522   mitochondrial respiration in defined coupling states. ROX is not necessarily equivalent to non-

523   mitochondrial respiration, considering oxygen-consuming reactions in mitochondria not related

524   to ET, such as oxygen consumption in reactions catalyzed by monoamine oxidases (type A and

525   B), monooxygenases (cytochrome P450 monooxygenases), dioxygenase (sulfur dioxygenase

526   and trimethyllysine dioxygenase), several hydoxylases, and more. Mitochondrial preparations,

527   especially those obtained from liver, may be contaminated by peroxisomes. This fact makes the

528   exact determination of mitochondrial oxygen consumption and mitochondria-associated

529   generation of reactive oxygen species complicated (Schönfeld *et al.* 2009). The dependence of

530   ROX-linked oxygen consumption needs to be studied in detail with respect to non-ET enzyme

531   activities, availability of specific substrates, oxygen concentration, and electron leakage leading

532   to the formation of reactive oxygen species.

533

534   *2.2. Coupling states and respiratory rates*

535   It is important to distinguish metabolic *pathways* from metabolic *states* and the

536   corresponding metabolic *rates*; for example: ET-pathways (**Fig. 6**), ET-state (**Fig. 5**), and ET-

537   capacity, *E*, respectively (**Table 1**). The protonmotive force is *high* in the OXPHOS-state when

538   it drives phosphorylation, *maximum* in the LEAK-state of coupled mitochondria, driven by

539   LEAK-respiration at a minimum back flux of protons to the matrix side, and *very low* in the

540   ET-state when uncouplers short-circuit the proton cycle (**Table 1**).

541

542 **Fig. 6. Four-compartment**
543 **model of oxidative**
544 **phosphorylation.** Respiratory
545 states (ET, OXPHOS, LEAK)
546 and corresponding rates (E, P, L)
547 are connected by the
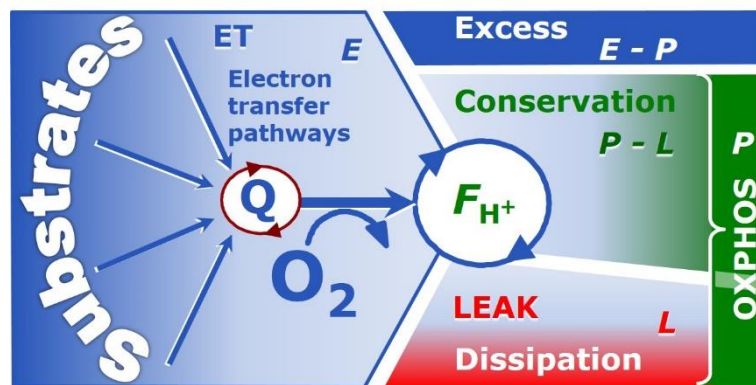
548 protonmotive force, $F_{H+\uparrow}$. Electron transfer-capacity, E, is partitioned into (*1*) dissipative

549 LEAK-respiration, L, when the capacity to perform work is irreversibly lost, (*2*) net OXPHOS-

550 capacity, P-L, with partial conservation of the capacity to perform work, and (*3*) the excess

551 capacity, E-P. Modified from Gnaiger (2014).

552

553   The three coupling states, ET, LEAK and OXPHOS, are shown schematically with the

554 corresponding respiratory rates, abbreviated as E, L and P, respectively (**Fig. 6**). E may exceed

555 or be equal to P, but E cannot theoretically be lower than P. $E < P$ must be discounted as an

556 artefact, which may be caused experimentally by: (*1*) loss of oxidative capacity during the time

557 course of the respirometric assay, since E is measured subsequently to P; (*2*) using insuffient

558 uncoupler concentrations; (*3*) using high uncoupler concentrations which inhibit ET (Gnaiger

559 2008); (*4*) high oligomycin concentrations applied for measurement of L before titrations of

560 uncoupler, when oligomycin exerts an inhibitory effect on E. On the other hand, the excess ET-

561 capacity is overestimated if non-saturating [ADP] or [P$_i$] are used. See State 3 in the next

562 section.

563       $E > P$ is observed in many types of mitochondria, varying between species, tissues and

564 cell types. It is the excess ET-capacity pushing the phosphorylation-flux (**Fig. 1B**) to the limit

565 of its *capacity of utilizing* the protonmotive force. Within any type of mitochondria, the

566 magnitude of $E > P$ depends on: (*1*) the pathway control state with single or multiple electron

567 input into the Q-junction and involvement of three or fewer coupling sites determining the

568 $H^+\uparrow/O_2$ *coupling stoichiometry* (**Fig. 1A**); and (*2*) the *biochemical coupling efficiency* expressed

569 as (*E-L*)/*E*, since an increase of *L* causes *P* to increase towards the limit of *E*. The *excess E-P*

570 *capacity*, *E-P*, therefore, provides a sensitive diagnostic indicator of specific injuries of the

571 phosphorylation-pathway, under conditions when *E* remains constant but *P* declines relative to

572 controls (**Fig. 6**). Substrate cocktails supporting simultaneous convergent electron transfer to

573 the Q-junction for reconstitution of tricarboxylic acid cycle (TCA cycle) function establish

574 pathway control states with high ET-capacity, and consequently increase the sensitivity of the

575 *E-P* assay.

576   When subtracting *L* from *P*, the dissipative LEAK component in the OXPHOS-state may

577 be overestimated. This can be avoided by measuring LEAK-respiration in a state when the

578 protonmotive force is adjusted to its slightly lower value in the OXPHOS-state, *e.g.*, by titration

579 of an ET inhibitor (Divakaruni and Brand 2011). Any turnover-dependent components of

580 proton leak and slip, however, are underestimated under these conditions (Garlid *et al.* 1993).

581 In general, it is inappropriate to use the term *ATP production* or *ATP turnover* for the difference

582 of oxygen consumption measured in states *P* and *L*. The difference *P-L* is the upper limit of the

583 part of OXPHOS-capacity that is freely available for ATP production (corrected for LEAK-

584 respiration) and is fully coupled to phosphorylation with a maximum mechanistic stoichiometry

585 (**Fig. 6**).

586

587 *2.3. Classical terminology for isolated mitochondria*

588   *'When a code is familiar enough, it ceases appearing like a code; one forgets that*

589   *there is a decoding mechanism. The message is identical with its meaning'*

590   (Hofstadter 1979).

591 Chance and Williams (1955; 1956) introduced five classical states of mitochondrial respiration

592 and cytochrome redox states. **Table 3** shows a protocol with isolated mitochondria in a closed

593 respirometric chamber, defining a sequence of respiratory states.

594
595
596

Table 3. Metabolic states of mitochondria (Chance and Williams, 1956; Table V).

State	$[O_2]$	ADP level	Substrate level	Respiration rate	Rate-limiting substance
1	>0	low	Low	slow	ADP
2	>0	high	~0	slow	substrate
3	>0	high	High	fast	respiratory chain
4	>0	low	High	slow	ADP
5	0	high	High	0	oxygen

597

598   **State 1** is obtained after addition of isolated mitochondria to air-saturated

599   isoosmotic/isotonic respiration medium containing inorganic phosphate, but no fuel substrates

600   and no adenylates, *i.e.*, AMP, ADP, ATP.

601   **State 2** is induced by addition of a high concentration of ADP (typically 100 to 300 µM),

602   which stimulates respiration transiently on the basis of endogenous fuel substrates and

603   phosphorylates only a small portion of the added ADP. State 2 is then obtained at a low

604   respiratory activity limited by zero endogenous fuel substrate availability (**Table 3**). If addition

605   of specific inhibitors of respiratory complexes, such as rotenone, does not cause a further

606   decline of oxygen consumption, State 2 is equivalent to residual oxygen consumption (See

607   below.). If inhibition is observed, undefined endogenous fuel substrates are a confounding

608   factor of pathway control by externally added substrates and inhibitors. In contrast to the

609   original protocol, an alternative sequence of titration steps is frequently applied, in which the

610   alternative State 2 has an entirely different meaning, when this second state is induced by

611   addition of fuel substrate without ADP (LEAK-state; in contrast to State 2 defined in **Table 2**

612   as a ROX state), followed by addition of ADP.

613   **State 3** is the state stimulated by addition of fuel substrates while the ADP concentration

614   is still high (**Table 3**) and supports coupled energy transformation through oxidative

615   phosphorylation. 'High ADP' is a concentration of ADP specifically selected to allow the

616   measurement of State 3 to State 4 transitions of isolated mitochondria in a closed respirometric

617   chamber. Repeated ADP titration re-establishes State 3 at 'high ADP'. Starting at oxygen

618   concentrations near air-saturation (ca. 200 µM O_2 at sea level and 37 °C), the total ADP

619   concentration added must be low enough (typically 100 to 300 µM) to allow phosphorylation

620   to ATP at a coupled rate of oxygen consumption that does not lead to oxygen depletion during

621   the transition to State 4. In contrast, kinetically-saturating ADP concentrations usually are an

622   order of magnitude higher than 'high ADP', *e.g.* 2.5 mM in isolated mitochondria. The

623   abbreviation State 3u is frequently used in bioenergetics, to indicate the state of respiration after

624   titration of an uncoupler, without sufficient emphasis on the fundamental difference between

625   OXPHOS-capacity (*well-coupled* with an *endogenous* uncoupled component) and ET-capacity

626   (*noncoupled*).

627   **State 4** is a LEAK-state that is obtained only if the mitochondrial preparation is intact

628   and well-coupled. Depletion of ADP by phosphorylation to ATP leads to a decline in the rate

629   of oxygen consumption in the transition from State 3 to State 4. Under these conditions, a

630   maximum protonmotive force and high ATP/ADP ratio are maintained, and the P»/O_2 ratio can

631   be calculated. State 4 respiration, L_T (**Table 1**), reflects intrinsic proton leak and intrinsic ATP

632   hydrolysis activity. Oxygen consumption in State 4 is an overestimation of LEAK-respiration

633   if the contaminating ATP hydrolysis activity recycles some ATP to ADP, $J_{P«}$, which stimulates

634   respiration coupled to phosphorylation, $J_{P»} > 0$. This can be tested by inhibition of the

635   phosphorylation-pathway using oligomycin, ensuring that $J_{P»} = 0$ (State 4o). Alternatively,

636   sequential ADP titrations re-establish State 3, followed by State 3 to State 4 transitions while

637   sufficient oxygen is available. However, anoxia may be reached before exhaustion of ADP

638   (State 5).

639   **State 5** is the state after exhaustion of oxygen in a closed respirometric chamber.

640   Diffusion of oxygen from the surroundings into the aqueous solution may be a confounding

641   factor preventing complete anoxia (Gnaiger 2001). Chance and Williams (1955) provide an

642   alternative definition of State 5, which gives it the meaning of ROX: 'State 5 may be obtained

643   by antimycin A treatment or by anaerobiosis'.

644   In **Table 3**, only States 3 and 4 (and 'State 2' in the alternative protocol without ADP;

645   not included in the table) are coupling control states, with the restriction that O_2 flux in State 3

646   may be limited kinetically by non-saturating ADP concentrations (**Table 1**).

647

648   **3. The protonmotive force and proton flux**

649   *3.1. Electric and chemical partial forces versus electrical and chemical units*

650   The protonmotive force across the mtIM (Mitchell 1961; Mitchell and Moyle 1967) was

651   introduced most beautifully in the *Grey Book 1966* (Mitchell 2011),

652                          $$\Delta p = \Delta\Psi + \Delta\mu_{H+}/F \qquad\qquad (Eq.\ 1)$$

653   The protonmotive force, Δp, consists of two partial forces: (*1*) The electrical part, $\Delta\Psi$, is the

654   difference of charge (electric potential difference), is not specific for H^+, and can, therefore, be

655   measured by the distribution of other permeable cations between the positive and negative

656   compartment (**Fig. 2**). (*2*) The chemical part, $\Delta\mu_{H+}$, is the chemical potential difference in H^+,

657   is proportional to the pH difference, and incorporates the Faraday constant (**Table 4**).

658   **Faraday constant**, $F = eN_A$ [C/mol] (**Table 4**, note 1) enables the conversion between

659   protonmotive force, $F_{H+/e} \equiv \Delta p$ [J/C], expressed per *motive charge*, e [C], and protonmotive

660   force or electrochemical potential difference, $F_{H+/n} \equiv \Delta\widetilde{\mu}_{H+} = \Delta p \cdot F$ [J/mol], expressed per

661   *motive amount of protons*, n [mol]. Proton charge, e, and amount of substance, n, are motive

662   entities expressed in units C and mol, respectively. Taken together, F is the conversion factor

663   for expressing protonmotive force and flux in motive units of e or n (Eq. 2; **Table 4**, Notes 1

664   and 2),

665                          $$F_{H+/n} = F_{H+/e} \cdot e \cdot N_A \qquad\qquad (Eq.\ 2.1)$$

666                          $$J_{H+/n} = J_{H+/e} / (e \cdot N_A) \qquad\qquad (Eq.\ 2.2)$$

667

Table 4. Protonmotive force and flux matrix. Columns: The protonmotive force is the sum of *partial isomorphic forces*, F_{el} and $F_{H+,d}$. Rows: Electrical and chemical formats (motive units MU, C and mol, for e and n, respectively). The Faraday constant, F, converts protonmotive force and flux from format e to n. In contrast to force (state), the conjugated flux (rate) cannot be partitioned.

State		**Force**		**Electric**	**+ chem.**	**Unit**	**Notes**
	Protonmotive force, e	Δp	$=$	$\Delta\Psi$	$+ \Delta\mu_{H+}/F$	$J \cdot C^{-1}$	1e
	Chemiosmotic potential, n	$\Delta\widetilde{\mu}_{H+}$	$=$	$\Delta\Psi \cdot F$	$+ \Delta\mu_{H+}$	$J \cdot mol^{-1}$	1n
State	**Isomorphic force**	F_{H+}		**El**	**+ H^+_d**	$J.MU^{-1}$	
	Electric charge, e	$F_{H+/e}$	$=$	$F_{el/e}$	$+ F_{H+,d/e}$	$J \cdot C^{-1}$	2e
	Amount of substance, n	$F_{H+/n}$	$=$	$F_{el/n}$	$+ F_{H+,d/n}$	$J \cdot mol^{-1}$	2n
Rate	**Isomorphic flux**	J_{H+}		**E** or	**n**	$MU \cdot s^{-1} \cdot m^{-3}$	
	Electric charge, e	$J_{H+/e}$		$J_{H+/e}$		$C \cdot s^{-1} \cdot m^{-3}$	3e
	Amount of substance, n	$J_{H+/n}$			$J_{H+/n}$	$mol \cdot s^{-1} \cdot m^{-3}$	3n

1: The Faraday constant, F, is the product of elementary charge ($e = 1.602\ 176\ 634 \cdot 10^{-19}$ C) and the Avogadro (Loschmidt) constant ($N_A = 6.022\ 140\ 76 \cdot 10^{23}$ mol^{-1}), $F = e \cdot N_A = 96{,}485.33$ C·mol^{-1} (Gibney 2017). F *is* the conversion factor between electrical and chemical units. $\Delta\widetilde{\mu}_{H+}$ is the chemiosmotic potential difference. 1e and 1n are the classical representations of 2e and 2n.

2: F_{H+} is the protonmotive force expressed in formats e or n, expressed in units C or mol. $F_{el/e} \equiv \Delta\Psi$ is the partial protonmotive force (el) acting generally on charged motive molecules (*i.e.* ions that are permeable across the mtIM). In contrast, $F_{H+,d/n} \equiv \Delta\mu_{H+}$ is the partial protonmotive force specific for proton diffusion, H^+_d. The sign of the force is negative for exergonic transformations in which exergy is lost or dissipated, $F_{H+\downarrow}$, and positive for endergonic transformations which conserve exergy in a coupled exergonic process, $F_{H+\uparrow} = -F_{H+\downarrow}$ (**Box 3**).

3: The sign of the flux, J_{H+}, depends on the definition of the compartmental direction of the translocation. For the outward direction, $J_{H+\uparrow}$, flux is positive since the direction involves formation of H$^+$ in the $^+$Compartment (H$^+\uparrow$ is added, $v_{H+\uparrow} = 1$; and H$^+\downarrow$ is removed, $v_{H+\downarrow} = -1$). Equally, $J_{H+\downarrow}$ is positive since the direction involves formation of H$^+$ in the $^-$Compartment (H$^+\downarrow$ is added, $v_{H+\downarrow} = 1$; and H$^+\uparrow$ is removed, $v_{H+\uparrow} = -1$; **Fig. 2**). The product of flux and force is volume-specific power [$J \cdot s^{-1} \cdot m^{-3} = W \cdot m^{-3}$]: $P_{V,H+} = J_{H+\uparrow/e} \cdot F_{H+\uparrow/e} = J_{H+\uparrow/n} \cdot F_{H+\uparrow/n}$.

691   In each format, the protonmotive force is expressed as the sum of two partial isomorphic

692   forces. The complex symbols in Eq. 1 can be explained and visualized more explicitly by

693   *partial isomorphic forces* as the components of the protonmotive force:

694   **Electric part of the protonmotive force:** (*1*) Isomorph *e*: $F_{el/e} \equiv \Delta\Psi$ is the electric part

695   of the protonmotive force expressed in electrical units joule per coulomb, *i.e.* volt [V = J/C].

696    $F_{el/e}$ is defined as partial Gibbs energy change per *motive elementary charge*, *e* [C], not specific

697   for proton charge (**Table 4**, Note 2*e*). (*2*) Isomorph *n*: $F_{el/n} \equiv \Delta\Psi{\cdot}F$ is the electric force expressed

698   in chemical units joule per mole [J/mol], defined as partial Gibbs energy change per *motive*

699   *amount of charge*, *n* [mol], not specific for proton charge (**Table 4**, Note 2*n*).

700

701   **Table 5. Power, exergy, force, flux, and advancement.**
702

Expression	Symbol	Definition	Unit	Notes
Power, volume-specific	$P_{V,tr}$	$P_{V,tr} = J_{tr} \cdot F_{tr} = d_{tr}G{\cdot}dt^{-1}$	$W{\cdot}m^{-3} =$ $J{\cdot}s^{-1}{\cdot}m^{-3}$	1
Force, isomorphic	F_{tr}	$F_{tr} = \partial G{\cdot}\partial_{tr}\xi^{-1}$	$J{\cdot}MU^{-1}$	2
Flux, isomorphic	J_{tr}	$J_{tr} = d_{tr}\xi{\cdot}dt^{-1}{\cdot}V^{-1}$	$MU{\cdot}s^{-1}{\cdot}m^{-3}$	3
Advancement, *n*	$d_{tr}\zeta_{H+/n}$	$d_{tr}\zeta_{H+/n} = d_{tr}n_{H+}{\cdot}\nu_{H+}^{-1}$	MU=mol	4*n*
Advancement, *e*	$d_{tr}\zeta_{H+/e}$	$d_{tr}\zeta_{H+/e} = d_{tr}e_{H+}{\cdot}\nu_{H+}^{-1}$	MU=C	4*e*
Electric partial force, *e*	$F_{el/e}$	$F_{el/e} \equiv \Delta\Psi =$ $RT/(zF){\cdot}\Delta\ln a_B$	$V = J{\cdot}C^{-1}$	5*e*
Electric partial force, *n*	$F_{el/n}$	$F_{el/n} \equiv \Delta\Psi{\cdot}zF =$ $RT{\cdot}\Delta\ln a_{Bz}$	$kJ{\cdot}mol^{-1}$	5*n*
at *z* = 1		$= 96.5{\cdot}\Delta\Psi$	$kJ{\cdot}mol^{-1}$	
Chemical partial force, *e*	$F_{H+,d/e}$	$F_{H+,d/e} \equiv \Delta\mu_{H+}/F =$ $-RT/F{\cdot}\ln(10){\cdot}\Delta pH$	$J{\cdot}C^{-1}$	6*e*
at 37 °C		$= -0.061{\cdot}\Delta pH$	$J{\cdot}C^{-1}$	
Chemical partial force, *n*	$F_{H+,d/n}$	$F_{H+,d/n} \equiv \Delta\mu_{H+} =$ $-RT{\cdot}\ln(10){\cdot}\Delta pH$	$J{\cdot}mol^{-1}$	6*n*
at 37 °C		$= -5.9{\cdot}\Delta pH$	$kJ{\cdot}mol^{-1}$	

703
704   1 to 4: A motive entity, expressed in a motive unit [MU] is a characteristic for any type of transformation,

705   tr. MU = mol or C in the chemical or electrical format of proton translocation.

706   2:   Isomorphic forces, F_{tr}, are related to the generalized forces, X_{tr}, of irreversible thermodynamics

707   as $F_{tr} = -X_{tr} \cdot T$, and the force of chemical reactions is the negative affinity, $F_r = -A$ (Prigogine 1967).

708   ∂G [J] is the partial Gibbs energy change in the advancement of transformation tr.

709   3:   For MU = C, flow is electric current, I_{el} [A = C·s^{-1}], vector flux is electric current density per area,

710   J_{el}, and compartmental flux is electric current density per volume, I_{el} [A·m^{-3}], all expressed in

711   electrical format.

712   4n: For a chemical reaction, the advancement of reaction r is $d_r\xi_B = d_r n_B \cdot v_B^{-1}$ [mol]. The stoichiometric

713   number is $v_B = -1$ or $v_B = 1$, depending on B being a product or substrate, respectively, in reaction

714   r involving one mole of B. The conjugated *intensive* molar quantity, $F_{B,r} = \partial G/\partial_r\xi_B$ [J·mol^{-1}], is the

715   chemical force of reaction or *reaction-motive* force per stoichiometric amount of B. In reaction

716   kinetics, $d_r n_B$ is expressed as a volume-specific quantity, which is the partial contribution to the

717   total concentration change of B, $d_r c_B = d_r n_B/V$ and $dc_B = dn_B/V$, respectively. In open systems with

718   constant volume V, $dc_B = d_r c_B + d_e c_B$, where r indicates the *internal* reaction and e indicates the

719   *external* flux of B into the unit volume of the system. At steady state the concentration does not

720   change, $dc_B = 0$, when $d_r c_B$ is compensated for by the external flux of B, $d_r c_B = -d_e c_B$ (Gnaiger

721   1993b). Alternatively, $dc_B = 0$ when B is held constant by different coupled reactions in which B

722   acts as a substrate or a product.

723   4e: Scalar potential difference across the mitochondrial membrane. In a scalar electric transformation

724   (flux of charge, *i.e.* volume-specific current, from the matrix space to the intermembrane and

725   extramitochondrial space) the motive force is the difference of charge (**Box 2**). The endergonic

726   direction of translocation is defined in **Fig. 2** as H$^+\downarrow \rightarrow$ H$^+\uparrow$.

727   5e: F = 96.5 (kJ·mol^{-1})/V. z_B is the charge number of ion B. a_B is the (relative) activity of ion B, which

728   in dilute solutions ($c < 0.1$ mol·dm^{-3}) is approximately equal to $c_B/c°$, where $c°$ is the standard

729   concentration of 1 mol·dm^{-3}. $\Delta\ln a_B = \ln a_2 - \ln a_1 = \ln(a_2/a_1)$, when ion B diffuses or is translocated

730   from compartment 1 to 2 (Eq. 4). Compartments 1 and 2 have to be defined in each case (**Fig.**

731   **2**). Note that ion selective electrodes (pH or TPP$^+$ electrodes) respond to $\ln a_B$. $\Delta\ln a_{H+} = -$

732        $\ln(10)\cdot\Delta$pH.

733   6: R = 8.31451 J·K^{-1}·mol^{-1} is the gas constant. RT = 2.479 and 2.579 kJ·mol^{-1} at 298.15 and 310.15

734   K (25 and 37 °C), respectively. See Eq. 3 and 4.

735   6e: $RT/F \cdot \Delta\ln a_{H+}$ yields force in the electrical format [J·C^{-1} = V]. RT/F = 2.479 and 2.579 mV at 298.15

736   and 310.15 K, respectively, and $\ln(10)\cdot RT/F$ = 59.16 and 61.54 mV, respectively.

737   *6n*:   *$RT \cdot \Delta \ln a_{H+}$ yields force in the chemical format [J·mol⁻¹]. ln(10)·RT = 5.708 and 5.938 kJ·mol⁻¹ at*

738   *298.15 and 310.15 K, respectively.*

739

740   **Chemical part of the protonmotive force:** (*1*) Isomorph *n*: $F_{H+,d/n} \equiv \Delta\mu_{H+}$ is the chemical

741 part (diffusion, displacement of H^+) of the protonmotive force expressed in units joule per mole

742 [J/mol]. $F_{H+,d/n}$ is defined as partial Gibbs energy change per *motive amount of protons, n* [mol]

743 (**Table 4**, Note 2*n*). (*2*) Isomorph *e*: $F_{H+,d/e} \equiv \Delta\mu_{H+}/F$ is the chemical force expressed in units

744 joule per coulomb [V], defined as partial Gibbs energy change per *motive amount of protons*

745 *expressed in units of electric charge, e* [C], but specific for proton charge (**Table 4**, Note 2*e*).

746   Protonmotive means that there is a potential for the movement of protons, and force is a

747 measure of the potential for motion. Motion is relative and not absolute (Principle of Galilean

748 Relativity); likewise there is no absolute potential, but isomorphic forces are potential

749 differences (**Table 5**, Notes 5 and 6),

750 $$F_{el/n} \;=\; \Delta\psi \cdot zF \;=\; RT \cdot \Delta \ln c_{Bz} \tag{Eq. 3.1}$$

751 $$F_{H+,d/n} \;=\; \Delta\mu_{H+} \;=\; RT \cdot \Delta \ln c_{H+} \tag{Eq. 3.2}$$

752 The isomorphism of the electric and chemical partial forces is clearly illustrated when

753 expressing all terms (Eq. 3) as dimensionless quantities (Eq. 4). For diffusion of protons into

754 the matrix space (**Fig. 2**),

755 $$F_{el\downarrow/n} \cdot RT^{-1} \;=\; \ln(c_{Bz\uparrow}/c_{Bz\downarrow}) \tag{Eq. 4.1}$$

756 $$F_{H+\downarrow,d/n} \cdot RT^{-1} \;=\; \ln(c_{H+\uparrow}/c_{H+\downarrow}) \tag{Eq. 4.2}$$

757   An electric partial force expressed in the format of electric charge, $F_{el\uparrow/e}$, of 0.2 V (**Table**

758 **5**, Note 5*e*) can be expressed equivalently in the format of amount, $F_{el\uparrow/n}$, of 19 kJ·mol⁻¹ $H^+\uparrow$

759 (Note 5*n*). For a ΔpH of 1 unit, the chemical partial force in the format of amount, $F_{H+\uparrow,d/n}$,

760 changes by 5.9 kJ·mol⁻¹ (**Table 5**, Note 6*n*) and chemical force in the format of charge $F_{H+\uparrow,d/e}$

761 changes by 0.06 V (Note 6*e*). Considering a driving force of -470 kJ·mol⁻¹ O_2 for oxidation, the

762   thermodynamic limit of the $H^+\uparrow/O_2$ ratio is reached at a value of $470/19 = 24$, compared to a

763   mechanistic stoichiometry of 20 (**Fig. 1**).

764

765   *3.2. Definitions*

766   **Control and regulation:** The terms metabolic *control* and *regulation* are frequently used

767   synonymously, but are distinguished in metabolic control analysis: 'We could understand the

768   regulation as the mechanism that occurs when a system maintains some variable constant over

769   time, in spite of fluctuations in external conditions (homeostasis of the internal state). On the

770   other hand, metabolic control is the power to change the state of the metabolism in response to

771   an external signal' (Fell 1997). Respiratory control may be induced by experimental control

772   signals that *exert* an influence on: (*1*) ATP demand and ADP phosphorylation-rate; (*2*) fuel

773   substrate composition, pathway competition; (*3*) available amounts of substrates and oxygen,

774   *e.g.*, starvation and hypoxia; (*3*) the protonmotive force, redox states, flux-force relationships,

775   coupling and efficiency; (*4*) Ca^{2+} and other ions including H^+; (*5*) inhibitors, *e.g.*, nitric oxide

776   or intermediary metabolites, such as oxaloacetate; (*6*) signalling pathways and regulatory

777   proteins, *e.g.* insulin resistance, transcription factor HIF-1 or inhibitory factor 1. *Mechanisms*

778   of respiratory control and regulation include adjustments of: (*1*) enzyme activities by allosteric

779   mechanisms and phosphorylation; (*2*) enzyme content, concentrations of cofactors and

780   conserved moieties (such as adenylates, nicotinamide adenine dinucleotide [NAD^+/NADH],

781   coenzyme Q, cytochrome *c*); (*3*) metabolic channeling by supercomplexes; and *(4)*

782   mitochondrial density (enzyme concentrations and membrane area) and morphology (cristae

783   folding, fission and fusion). (*5*) Mitochondria are targeted directly by hormones, thereby

784   affecting their energy metabolism (Lee *et al.* 2013; Gerö and Szabo 2016; Price and Dai 2016;

785   Moreno *et al.* 2017). Evolutionary or acquired differences in the genetic and epigenetic basis

786   of mitochondrial function (or dysfunction) between subjects and gene therapy; age; gender,

787   biological sex, and hormone concentrations; life style including exercise and nutrition; and

788 environmental issues including thermal, atmospheric, toxicological and pharmacological

789 factors, exert an influence on all control mechanisms listed above. For reviews, see Brown

790 1992; Gnaiger 1993a, 2009; 2014; Paradies *et al.* 2014; Morrow *et al.* 2017.

791 **Respiratory control and response:** Lack of control by a metabolic pathway, *e.g.*

792 phosphorylation-pathway, does mean that there will be no response to a variable activating it,

793 *e.g.* [ADP]. However, the reverse is not true as the absence of a response to [ADP] does not

794 exclude the phosphorylation-pathway from having some degree of control. The degree of

795 control of a component of the OXPHOS-pathway on an output variable, such as oxygen flux,

796 will in general be different from the degree of control on other outputs, such as phosphorylation-

797 flux or proton leak flux (**Box 2**). As such, it is necessary to be specific as to which input and

798 output are under consideration (Fell 1997). Therefore, the term respiratory control is elaborated

799 in more detail in the following section.

800 **Respiratory coupling control:** Respiratory control refers to the ability of mitochondria

801 to adjust oxygen consumption in response to external control signals by engaging various

802 mechanisms of control and regulation. Respiratory control is monitored in a mitochondrial

803 preparation under conditions defined as respiratory states. When phosphorylation of ADP to

804 ATP is stimulated or depressed, an increase or decrease is observed in electron flux linked to

805 oxygen consumption in respiratory coupling states of intact mitochondria ('controlled states' in

806 the classical terminology of bioenergetics). Alternatively, coupling of electron transfer with

807 phosphorylation is disengaged by disruption of the integrity of the mtIM or by uncouplers,

808 functioning like a clutch in a mechanical system. The corresponding coupling control state is

809 characterized by high levels of oxygen consumption without control by phosphorylation

810 ('uncontrolled state'). Energetic coupling is defined in **Box 4**. Loss of coupling lowers the

811 efficiency by intrinsic uncoupling and decoupling, or pathological dyscoupling. Such

812 generalized uncoupling is different from switching to mitochondrial pathways that involve

813 fewer than three proton pumps ('coupling sites': Complexes CI, CIII and CIV), bypassing CI

814   through multiple electron entries into the Q-junction (**Fig. 1**). A bypass of CIII and CIV is

815   provided by alternative oxidases, which reduce oxygen without proton translocation.

816   Reprogramming of mitochondrial pathways may be considered as a switch of gears (changing

817   the stoichiometry) rather than uncoupling (loosening the stoichiometry).

818   **Pathway control states** are obtained in mitochondrial preparations by depletion of

819   endogenous substrates and addition to the mitochondrial respiration medium of fuel substrates

820   (CHNO) and specific inhibitors, activating selected mitochondrial pathways (**Fig. 1**). Coupling

821   control states and pathway control states are complementary, since mitochondrial preparations

822   depend on an exogenous supply of pathway-specific fuel substrates and oxygen (Gnaiger 2014).

823

824   **Box 2: Metabolic fluxes and flows: vectorial and scalar**

825   In mitochondrial electron transfer (**Fig. 1**), vectorial transmembrane proton flux is coupled

826   through the proton pumps CI, CIII and CIV to the catabolic flux of scalar reactions, collectively

827   measured as oxygen flux. In **Fig. 2**, the scalar catabolic reaction, k, of oxygen consumption,

828     $J_{O_2,k}$ [mol·s^{-1}·m^{-3}], is expressed as oxygen flux per volume, V [m^3], of the instrumental chamber

829   (the system).

830   Fluxes are *vectors*, if they have *spatial* direction in addition to magnitude. A vector flux

831   (surface-density of flow) is expressed per unit cross-sectional area, A [m^2], perpendicular to the

832   direction of flux. If *flows, I,* are defined as extensive quantities of the *system*, as vector or scalar

833   flow, $\boldsymbol{I}$ or I [mol·s^{-1}], respectively, then the corresponding vector and scalar *fluxes, J,* are

834   obtained as $\boldsymbol{J} = \boldsymbol{I} \cdot A^{-1}$ [mol·s^{-1}·m^{-2}] and $J = I \cdot V^{-1}$ [mol·s^{-1}·m^{-3}], respectively, expressing flux as an

835   area-specific vector or volume-specific scalar quantity.

836   Vectorial transmembrane proton fluxes, $J_{H+\uparrow}$ and $J_{H+\downarrow}$, are analyzed in a heterogenous

837   compartmental system as a quantity with *directional* but not *spatial* information. Translocation

838   of protons across the mtIM has a defined direction, either from the negative compartment

839   (matrix space; negative or $^-$Compartment) to the positive compartment (inter-membrane space;

840   positive or $^+$Compartment) or *vice versa* (**Fig. 2**). The arrows defining the direction of the

841   translocation between the two compartments may point upwards or downwards, right or left,

842   without any implication that these are actual directions in space. The $^+$Compartment is neither

843   above nor below the $^-$Compartment in a spatial sense, but can be visualized arbitrarily in a figure

844   in the upper position (**Fig. 2**). In general, the *compartmental direction* of vectorial translocation

845   from the $^-$Compartment to the $^+$Compartment is defined by assigning the initial and final state

846   as *ergodynamic compartments*, $H^+\downarrow \rightarrow H^+\uparrow$ or $0 = -H^+\downarrow + H^+\uparrow$, related to work (erg = work) that

847   must be performed to lift the proton from a lower to a higher electrochemical potential or from

848   the lower to the higher ergodynamic compartment (Gnaiger 1993b).

849   In direct analogy to *vectorial* translocation, the direction of a *scalar* chemical reaction, A

850     $\rightarrow$ B or $0 = -A+B$, is defined by assigning substrates and products, A and B, as ergodynamic

851   compartments. O_2 is defined as a substrate in respiratory O_2 consumption, which together with

852   the fuel substrates comprises the substrate compartment of the catabolic reaction (**Fig. 2**).

853   Volume-specific scalar O_2 flux is coupled (**Box 4**) to vectorial translocation. In order to

854   establish a quantitative relation between the coupled fluxes, both $J_{O_2,k}$ and $J_{H^+\uparrow}$ must be

855   expressed in identical units, $[\text{mol·s}^{-1}\text{·m}^{-3}]$ or $[\text{C·s}^{-1}\text{·m}^{-3}]$, yielding the $H^+\uparrow/O_2$ ratio (**Fig. 1**). The

856   *vectorial* proton flux in compartmental translocation has *compartmental direction*,

857   distinguished from a *vector* flux with *spatial direction*. Likewise, the corresponding

858   protonmotive force is defined as an electrochemical potential *difference* between two

859   compartments, in contrast to a *gradient* across the membrane or a vector force with defined

860   spatial direction.

861

---

862   **The steady-state:** Mitochondria represent a thermodynamically open system functioning

863   as a biochemical transformation system in non-equilibrium states. State variables (protonmotive

864   force; redox states) and metabolic fluxes (*rates*) are measured in defined mitochondrial

865   respiratory *states*. Strictly, steady states can be obtained only in open systems, in which changes

866   due to *internal* transformations, *e.g.*, O_2 consumption, are instantaneously compensated for by

867   *external* fluxes *e.g.*, O_2 supply, such that oxygen concentration does not change in the system

868   (Gnaiger 1993b). Mitochondrial respiratory states monitored in closed systems satisfy the

869   criteria of pseudo-steady states for limited periods of time, when changes in the system

870   (concentrations of O_2, fuel substrates, ADP, P_i, H^+) do not exert significant effects on metabolic

871   fluxes (respiration, phosphorylation). Such pseudo-steady states require respiratory media with

872   sufficient buffering capacity and kinetically-saturating concentrations of substrates to be

873   maintained, and thus depend on the kinetics of the processes under investigation. Proton

874   turnover, $J_{\infty H+}$, and ATP turnover, $J_{\infty P}$, proceed in the steady-state at constant $F_{H+\uparrow}$, when $J_{H+\infty}$

875    $= J_{H+\uparrow} = J_{H+\downarrow}$, and at constant $F_{P»}$, when $J_{P\infty} = J_{P»} = J_{P«}$ (**Fig. 2**).

876

877   **Box 3: Endergonic and exergonic transformations, exergy and dissipation**

878   A chemical reaction, or any transformation, is exergonic if the Gibbs energy change (exergy)

879   of the reaction is negative at constant temperature and pressure. The sum of Gibbs energy

880   changes of all internal transformations in a system can only be negative, *i.e.* exergy is

881   irreversibly dissipated. Endergonic reactions are characterized by positive Gibbs energies of

882   reaction and cannot proceed spontaneously in the forward direction as defined. For instance,

883   the endergonic reaction P» is coupled to exergonic catabolic reactions, such that the total Gibbs

884   energy change is negative, *i.e.* exergy must be dissipated for the reaction to proceed (**Fig. 2**).

885   In contrast, energy cannot be lost or produced in any internal process, which is the key

886   message of the first law of thermodynamics. Thus mitochondria are the sites of energy

887   transformation but not energy production. Open and closed systems can gain energy and exergy

888   only by external fluxes, *i.e.* uptake from the environment. Exergy is the potential to perform

889   work. In the framework of flux-force relationships (**Box 4**), the *partial* derivative of Gibbs

890   energy per advancement of a transformation is an isomorphic force, F_{tr} (**Table 5**, Note 2). In

891   other words, force is equal to exergy per motive entity (in integral form, this definition takes

892 care of non-isothermal processes). This formal generalization represents an appreciation of the

893 conceptual beauty of Peter Mitchell's innovation of the protonmotive force against the

894 background of the established paradigm of the electromotive force (emf) defined at the limit of

895 zero current (Cohen *et al.* 2008).

896

3.3. Forces and fluxes in physics and thermodynamics

898 According to its definition in physics, a potential difference and as such the

899 *protonmotive force*, Δp, is not a force *per se* (Cohen *et al.* 2008). The fundamental forces of

900 physics are distinguished from *motive forces* of statistical and irreversible thermodynamics.

901 Complementary to the attempt towards unification of fundamental forces defined in physics,

902 the concepts of Nobel laureates Lars Onsager, Erwin Schrödinger, Ilya Prigogine and Peter

903 Mitchell (even if expressed in apparently unrelated terms) unite the diversity of *generalized* or

904 'isomorphic' *flux-force* relationships, the product of which links to entropy production and the

905 Second Law of thermodynamics (Schrödinger 1944; Prigogine 1967). A *motive force* is the

906 derivative of potentially available or 'free' energy (exergy) per *motive entity* (**Box 3**). Perhaps

907 the first account of a *motive force* in energy transformation can be traced back to the Peripatetic

908 school around 300 BC in the context of moving a lever, up to Newton's motive force

909 proportional to the alteration of motion (Coopersmith 2010). As a generalization, isomorphic

910 motive forces are considered as *entropic forces* in physics (Wang 2010).

911 **Vectorial and scalar forces, and fluxes:** In chemical reactions and osmotic or diffusion

912 processes occurring in a closed heterogeneous system, such as a chamber containing isolated

913 mitochondria, scalar transformations occur without measured spatial direction but between

914 separate compartments (translocation between the matrix and intermembrane space) or between

915 energetically-separated chemical substances (reactions from substrates to products). Hence, the

916 corresponding fluxes are not vectorial but scalar, and are expressed per volume and not per

917 membrane area (**Box 2**). The corresponding motive forces are also scalar potential *differences*

918 across the membrane (**Table 5**), without taking into account the *gradients* across the 6 nm thick

919 mtIM (Rich 2003).

920 **Coupling:** In energetics (ergodynamics), coupling is defined as an energy transformation

921 fuelled by an exergonic (downhill) input process driving the advancement of an endergonic

922 (uphill) output process. The (negative) output/input power ratio is the efficiency of a coupled

923 energy transformation (**Box 4**). At the limit of maximum efficiency of a completely coupled

924 system, the (negative) input power equals the (positive) output power, such that the total power

925 approaches zero at the maximum efficiency of 1, and the process becomes fully reversible

926 without any dissipation of exergy, *i.e.* without entropy production.

927

928 **Box 4: Coupling, power and efficiency, at constant temperature and pressure**

929 Energetic coupling means that two processes of energy transformation are linked such that the

930 input power, P_{in}, is the driving element of the output power, P_{out}, and the out/input power ratio

931 is the efficiency. In general, power is work per unit time [$J \cdot s^{-1}$ = W]. When describing a system

932 with volume V without information on the internal structure, the output is defined as the *external*

933 work (exergy) performed by the *total* system on its environment. Such a system may be open

934 for any type of exchange, or closed and thus allowing only heat and work to be exchanged

935 across the system boundaries. This is the classical black box approach of thermodynamics. In

936 contrast, in a colourful compartmental analysis of *internal* energy transformations (**Fig. 2**), the

937 system is structured and described by definition of ergodynamic compartments (with

938 information on the heterogeneity of the system; **Box 2**) and analysis of separate parts, *i.e.* a

939 sequence of *partial* energy transformations, tr. At constant temperature and pressure, power per

940 unit volume, $P_{V,tr} = P_{tr}/V$ [$W \cdot m^{-3}$], is the product of a volume-specific flux, J_{tr}, and its conjugated

941 force, F_{tr}, and is directly linked to entropy production, $d_i S/dt = \Sigma_{tr} P_{tr}/T$ [$W \cdot K^{-1}$], as generalized

942 by irreversible thermodynamics (Prigogine 1967; Gnaiger 1993a,b). Output power of proton

943 translocation and catabolic input power are (**Fig. 2**),

944   Output: $P_{H+\uparrow}/V = J_{H+\uparrow} \cdot F_{H+\uparrow}$

945   Input: $P_k/V = J_{O_2,k} \cdot F_{O_2,k}$

946     $F_{O_2,k}$ is the exergonic input force with a negative sign, and, $F_{H+\uparrow}$, is the endergonic output force

947   with a positive sign (**Box 3**). Ergodynamic efficiency is the ratio of output/input power, or the

948   flux ratio times force ratio (Gnaiger 1993a,b),

949
$$\varepsilon = \frac{P_{H+\uparrow}}{-P_k} = \frac{J_{H+\uparrow}}{J_{O_2,k}} \cdot \frac{F_{H+\uparrow}}{-F_{O_2,k}}$$

950   The concept of incomplete coupling relates exclusively to the first term, *i.e.* the flux ratio, or

951     $H^+\uparrow/O_2$ ratio (**Fig. 1**). Likewise, respirometric definitions of the $P\gg/O_2$ ratio and biochemical

952   coupling efficiency (Section 3.2) consider flux ratios. In a completely coupled process, the

953   power efficiency, ε, depends entirely on the force ratio, ranging from zero efficiency at an

954   output force of zero, to the limiting output force and maximum efficiency of 1.0, when the total

955   power of the coupled process, $P_t = P_k + P_{H+\uparrow}$, equals zero, and any net flows are zero at

956   ergodynamic equilibrium of a coupled process. Thermodynamic equilibrium is defined as the

957   state when all potentials (all forces) are dissipated and equilibrate towards their minima of zero.

958   In a fully or completely coupled process, output and input fluxes are directly proportional in a

959   fixed ratio technically defined as a stoichiometric relationship (a gear ratio in a mechanical

960   system). Such maximal stoichiometric output/input flux ratios are considered in OXPHOS

961   analysis as the upper limits or mechanistic $H^+\uparrow/O_2$ and $P\gg/O_2$ ratios (**Fig. 1**).

962

963   **Coupled versus bound processes:** Since the chemiosmotic theory describes the

964   mechanisms of coupling in OXPHOS, it may be interesting to ask if the electrical and chemical

965   parts of proton translocation are coupled processes. This is not the case according to the

966   definition of coupling. If the coupling mechanism is disengaged, the output process becomes

967   independent of the input process, and both proceed in their downhill (exergonic) direction (**Fig.**

968   **2**). It is not possible to physically uncouple the electrical and chemical processes, which are

969   only *theoretically* partitioned as electrical and chemical components. The electrical and

970   chemical partial protonmotive *forces*, $F_{el\uparrow}$ and $F_{H+\uparrow,d}$, can be measured separately. In contrast,

971   the corresponding proton *flux*, $J_{H+\uparrow}$, is non-separable, *i.e.*, cannot be uncoupled. Then these are

972   not *coupled* processes, but are defined as *bound* processes. The electrical and chemical parts

973   are tightly bound partial forces, since the flux cannot be partitioned but expressed only in either

974   an electrical or chemical format, $J_{H+/e}$ or $J_{H+/n}$ (**Table 4**).

975

976   **4. Normalization: fluxes and flows**

977   The challenges of measuring mitochondrial respiratory flux are matched by those of

978   normalization, whereby O_2 consumption may be considered as the numerator and normalization

979   as the complementary denominator, which are tightly linked in reporting the measurements in

980   a format commensurate with the requirements of a database.

981

982   *4.1. Flux per chamber volume*

983   When the reactor volume does not change during the reaction, which is typical for liquid

984   phase reactions, the volume-specific *flux of a chemical reaction* r is the time derivative of the

985   advancement of the reaction per unit volume, $J_{V,B} = d_r\xi_B/dt \cdot V^{-1}$ [$(mol \cdot s^{-1}) \cdot L^{-1}$]. The *rate of*

986   *concentration change* is dc_B/dt [$(mol \cdot L^{-1}) \cdot s^{-1}$], where concentration is $c_B = n_B/V$. It is helpful to

987   make the subtle distinction between [$mol \cdot s^{-1} \cdot L^{-1}$] and [$mol \cdot L^{-1} \cdot s^{-1}$] for the fundamentally

988   different quantities of volume-specific flux and rate of concentration change, which merge to a

989   single expression only in closed systems. In open systems, external fluxes (such as O_2 supply)

990   are distinguished from internal transformations (metabolic flux, O_2 consumption). In a closed

991   system, external flows of all substances are zero and O_2 consumption (internal flow), I_{O_2}

992   [$pmol \cdot s^{-1}$], causes a decline of the amount of O_2 in the system, n_{O_2} [nmol]. Normalization of

993   these quantities for the volume of the system, V [$L = dm^3$], yields volume-specific O_2 flux, J_{V,O_2}

994    $= I_{O_2}/V$ [$nmol \cdot s^{-1} \cdot L^{-1}$], and O_2 concentration, [O_2] or $c_{O_2} = n_{O_2}/V$ [$nmol \cdot mL^{-1} = \mu mol \cdot L^{-1} = \mu M$].

995   Instrumental background O_2 flux is due to external flux into a non-ideal closed respirometer,

996   such that total volume-specific flux has to be corrected for instrumental background O_2 flux,

997   *i.e.* O_2 diffusion into or out of the instrumental chamber. J_{V,O_2} is relevant mainly for

998   methodological reasons and should be compared with the accuracy of instrumental resolution

999   of background-corrected flux, *e.g.* ± 1 nmol$\cdot$s$^{-1}\cdot$L^{-1} (Gnaiger 2001). 'Metabolic' or catabolic

1000   indicates O_2 flux, $J_{O_2,k}$, corrected for instrumental background O_2 flux and chemical background

1001 O_2 flux due to autoxidation of chemical components added to the incubation medium.

1002

1003   *4.2. System-specific and sample-specific normalization*

1004   Application of common and generally defined units is required for direct transfer of

1005   reported results into a database. The second [s] is the *SI* unit for the base quantity *time*. It is also

1006   the standard time-unit used in solution chemical kinetics. **Table 6** lists some conversion factors

1007   to obtain *SI* units. The term *rate* is not sufficiently defined to be useful for a database (**Fig. 7**).

1008   The inconsistency of the meanings of rate becomes fully apparent when considering Galileo

1009   Galilei's famous principle, that 'bodies of different weight all fall at the same rate (have a

1010   constant acceleration)' (Coopersmith 2010).

1011   **Extensive quantities:** An extensive quantity increases proportionally with system size.

1012   The magnitude of an extensive quantity is completely additive for non-interacting subsystems,

1013   such as mass or flow expressed per defined system. The magnitude of these quantities depends

1014   on the extent or size of the system (Cohen *et al.* 2008).

1015   **Size-specific quantities:** 'The adjective *specific* before the name of an extensive quantity

1016   is often used to mean *divided by mass*' (Cohen *et al.* 2008). Mass-specific flux is flow divided

1017   by mass of the system. A mass-specific quantity is independent of the extent of non-interacting

1018   homogenous subsystems. Tissue-specific quantities are of fundamental interest in comparative

1019   mitochondrial physiology, where *specific* refers to the *type* rather than *mass* of the tissue. The

1020   term *specific*, therefore, must be further clarified, such that tissue mass-specific, *e.g.*, muscle

1021   mass-specific quantities are defined.

1022

1023   **Fig. 7. Different meanings of**

1024   *rate* **may lead to confusion, if**

1025   **the   normalization   is   not**

1026   **sufficiently   specified.**   Results

1027   are frequently expressed as mass-

1028   specific *flux*, J_m, per mg protein,

1029   dry or wet weight (mass). Cell

Flow, I [mol·s^{-1}] per system
(extensive)

J_V [mol·s^{-1}·m^{-3}]
Method: per volume

Rate → Flux, J

J_m [mol·s^{-1}·kg^{-1}]
Results (specific):
per mass

Turnover rate [s^{-1}]

Flux control ratio, *FCR*
I_{low}/I_{high} or J_{low}/J_{high}

1030   volume, V_{cell}, or mitochondrial volume, V_{mt}, may be used for normalization (volume-specific

1031   flux, J_{Vcell} or J_{Vmt}), which then must be clearly distinguished from flux, J_V, expressed for

1032   methodological reasons per volume of the measurement system, or flow per cell, I_X.

1033

1034   **Molar quantities:** 'The adjective *molar* before the name of an extensive quantity

1035   generally means *divided by amount of substance*' (Cohen *et al.* 2008). The notion that all molar

1036   quantities then become *intensive* causes ambiguity in the meaning of *molar Gibbs energy*. It is

1037   important to emphasize the fundamental difference between normalization for amount of

1038   substance *in a system* or for amount of motive substance *in a transformation*. When the Gibbs

1039   energy of a system, G [J], is divided by the amount of substance B in the system, n_B [mol], a

1040   *size-specific* molar quantity is obtained, $G_B = G/n_B$ [J·mol^{-1}], which is not any force at all. In

1041   contrast, when the partial Gibbs energy change, ∂G [J], is divided by the motive amount of

1042   substance B in reaction r (advancement of reaction), $\partial_r\xi_B$ [mol], the resulting intensive molar

1043   quantity, $F_{B,r} = \partial G/\partial_r\xi_B$ [J·mol^{-1}], is the chemical motive force of reaction r involving 1 mol B

1044   (**Table 5**, Note 4).
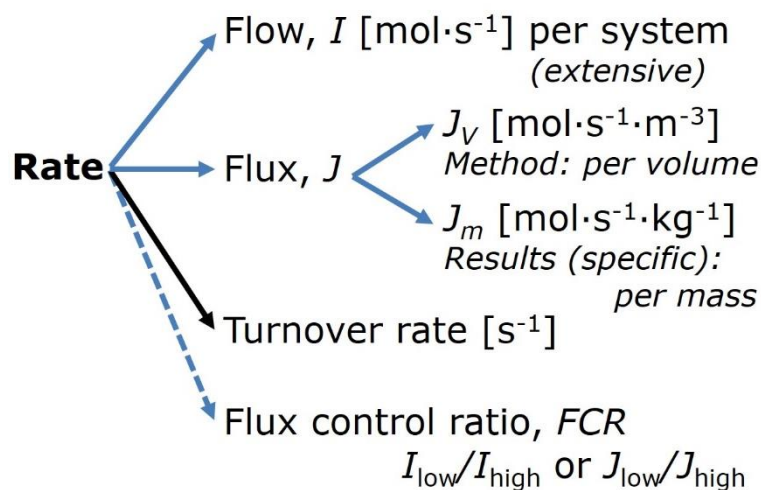
1045   **Flow per system, *I*:** In analogy to electrical terms, flow as an extensive quantity (*I*; per

1046   system) is distinguished from flux as a size-specific quantity (*J*; per system size) (**Fig. 7**).

1047   Electric current is flow, I_{el} [A = C·s^{-1}] per system (extensive quantity). When dividing this

1048   extensive quantity by system size (membrane area), a size-specific quantity is obtained, which

1049   is electric flux (electric current density), J_{el} [A·m^{-2} = C·s^{-1}·m^{-2}].

1050

1051
1052   **Table 6. Sample concentrations and normalization of flux with *SI* base units.**

Expression	Symbol	Definition	*SI* Unit	Notes
Sample				
Identity of sample	*X*	Cells, animals, patients		
Number of sample entities *X*	N_X	Number of cells, *etc.*	x	
Mass of sample *X*	m_X		kg	1
Mass of entity *X*	M_X	$M_X = m_X \cdot N_X^{-1}$	kg·x^{-1}	1
Mitochondria				
Mitochondria	mt	X = mt		
Amount of mt-elements	mte	Quantity of mt-marker	x$_{mte}$	
Concentrations				
Sample number concentration	C_{NX}	$C_{NX} = N_X \cdot V^{-1}$	x·m^{-3}	2
Sample mass concentration	C_{mX}	$C_{mX} = m_X \cdot V^{-1}$	kg·m^{-3}	
Mitochondrial concentration	C_{mte}	$C_{mte} = $ mte·V^{-1}	x$_{mte}$·m^{-3}	3
Specific mitochondrial density	D_{mte}	$D_{mte} = $ mte·m_X^{-1}	x$_{mte}$·kg^{-1}	4
Mitochondrial content, mte per entity *X*	mte$_X$	mte$_X$ = mte·N_X^{-1}	x$_{mte}$·x^{-1}	5
O$_2$ flow and flux				6
Flow	I_{O_2}	Internal flow	mol·s^{-1}	7
Volume-specific flux	J_{V,O_2}	$J_{V,O_2} = I_{O_2} \cdot V^{-1}$	mol·s^{-1}·m^{-3}	8
Flow per sample entity *X*	I_{X,O_2}	$I_{X,O_2} = J_{V,O_2} \cdot C_{NX}^{-1}$	mol·s^{-1}·x^{-1}	9
Mass-specific flux	J_{mX,O_2}	$J_{mX,O_2} = J_{V,O_2} \cdot C_{mX}^{-1}$	mol·s^{-1}·kg^{-1}	
Mitochondria-specific flux	J_{mte,O_2}	$J_{mte,O_2} = J_{V,O_2} \cdot C_{mte}^{-1}$	mol·s^{-1}·x$_{mte}^{-1}$	10

1053
1054   1   The *SI* prefix k is used for the SI base unit of mass (kg = 1,000 g). In praxis, various *SI* prefixes are

1055   used for convenience, to make numbers easily readable, *e.g.* 1 mg tissue, cell or mitochondrial mass

1056   instead of 0.000001 kg.

1057   2   In case *X* = cells, the sample number concentration is $C_{Ncell} = N_{cell} \cdot V^{-1}$, and volume may be expressed

1058   in [dm^3 = L] or [cm^3 = mL]. See **Table 7** for different sample types.

1059   3   mt-concentration is an experimental variable, dependent on sample concentration: (*1*) $C_{mte} = $ mte·V^{-1};

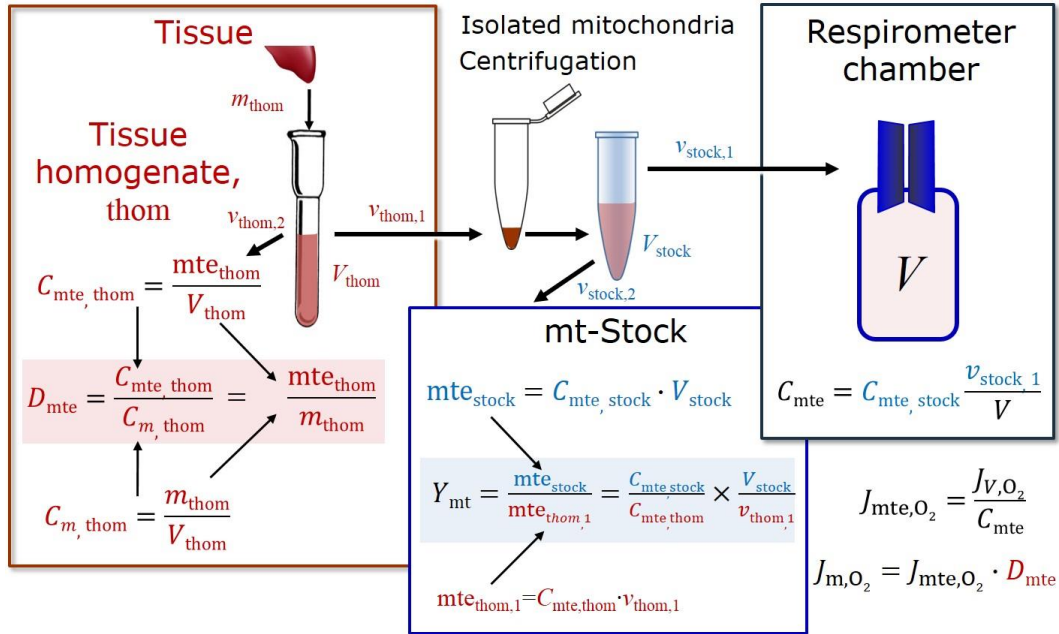1060   (*2*) $C_{mte} = $ mte$_X$·C_{NX}; (*3*) $C_{mte} = C_{mX} \cdot D_{mte}$.

1061   4 If the amount of mitochondria, mte, is expressed as mitochondrial mass, then D_{mte} is the mass

1062   fraction of mitochondria in the sample. If mte is expressed as mitochondrial volume, V_{mt}, and the

1063   mass of sample, m_X, is replaced by volume of sample, V_X, then D_{mte} is the volume fraction of

1064   mitochondria in the sample.

1065   5 $mte_X = mte \cdot N_X^{-1} = C_{mte} \cdot C_{NX}^{-1}$.

1066   6 O_2 can be replaced by other chemicals B to study different reactions, *e.g.* ATP, H_2O_2, or

1067   compartmental translocations, *e.g.* Ca^{2+}.

1068   7 I_{O_2} and V are defined per instrument chamber as a system of constant volume (and constant

1069   temperature), which may be closed or open. I_{O_2} is abbreviated for $I_{O_2,r}$, *i.e.* the metabolic or internal

1070 O_2 flow of the chemical reaction r in which O_2 is consumed, hence the negative stoichiometric

1071   number, $v_{O_2} = -1$. $I_{O_2,r} = d_r n_{O_2} / dt \cdot v_{O_2}^{-1}$. If r includes all chemical reactions in which O_2 participates, then

1072 $d_r n_{O_2} = dn_{O_2} - d_e n_{O_2}$, where dn_{O_2} is the change in the amount of O_2 in the instrument chamber and $d_e n_{O_2}$

1073   is the amount of O_2 added externally to the system. At steady state, by definition $dn_{O_2} = 0$, hence $d_r n_{O_2}$

1074 $= -d_e n_{O_2}$.

1075   8 J_{V,O_2} is an experimental variable, expressed per volume of the instrument chamber.

1076   9 I_{X,O_2} is a physiological variable, depending on the size of entity X.

1077   10 There are many ways to normalize for a mitochondrial marker, that are used in different experimental

1078   approaches: *(1)* $J_{mte,O_2} = J_{V,O_2} \cdot C_{mte}^{-1}$; *(2)* $J_{mte,O_2} = J_{V,O_2} \cdot C_{mX}^{-1} \cdot D_{mte}^{-1} = J_{mX,O_2} \cdot D_{mte}^{-1}$; *(3)* $J_{mte,O_2} = J_{V,O_2} \cdot C_{NX}^{-1} \cdot mte_X^{-1}$

1079 $= I_{X,O_2} \cdot mte_X^{-1}$; *(4)* $J_{mte,O_2} = I_{O_2} \cdot mte^{-1}$.

1080

1081   **Size-specific flux, *J***: Metabolic O_2 flow per tissue increases as tissue mass is increased.

1082 Tissue mass-specific O_2 flux should be independent of the size of the tissue sample studied in

1083 the instrument chamber, but volume-specific O_2 flux (per volume of the instrument chamber,

1084 *V*) should increase in direct proportion to the amount of sample in the chamber. Accurate

1085 definition of the experimental system is decisive: whether the experimental chamber is the

1086 closed, open, isothermal or non-isothermal *system* with defined volume as part of the

1087 measurement apparatus, in contrast to the experimental *sample* in the chamber (**Table 6**).

1088 Volume-specific O_2 flux depends on mass-concentration of the sample in the chamber, but

1089 should be independent of the chamber volume. There are practical limitations to increasing the

1090 mass-concentration of the sample in the chamber, when one is concerned about crowding

1091 effects and instrumental time resolution.

1092

1093

1094

1095 **Fig. 8. Normalization of volume-specific flux of isolated mitochondria and**

1096 **tissue homogenate. A:** Mitochondrial yield, Y_{mt}, in preparation of isolated

1097 mitochondria. $v_{thom,1}$ and $v_{stock,1}$ are the volumes transferred from the total volume,

1098 V_{thom} and V_{stock}, respectively. $mte_{thom,1}$ is the amount of mitochondrial elements in

1099 volume $v_{thom,1}$ used for isolation. **B:** In respirometry with homogenate, $v_{thom,1}$ is

1100   transferred directly into the respirometer chamber. See **Table 6** for further

1101   explanation of symbols.

1102

1103   **Sample concentration C_{mX}:** Normalization for sample concentration is required for

1104   reporting respiratory data. Consider a tissue or cells as the sample, X, and the sample mass, m_X

1105   [mg] from which a mitochondrial preparation is obtained. The sample mass, m_X, is frequently

1106   measured as wet or dry weight, W_w or W_d [mg], or as amount of tissue or cell protein, $m_{Protein}$.

1107   In the case of permeabilized tissues, cells, and homogenates, the sample concentration, $C_{mX} =$

1108 m_X/V [mg·mL^{-1} = g·L^{-1}], is simply the mass of the subsample of tissue that is transferred into

1109   the instrument chamber. Part of the mitochondria from the tissue is lost during preparation of

1110   isolated mitochondria, and only a fraction of mitochondria is obtained, expressed as the

1111   mitochondrial yield (**Fig. 8**). At a high mitochondrial yield the sample of isolated mitochondria

1112   is more representative of the total mitochondrial population than in preparations characterized

1113   by low mitochondrial yield. Determination of the mitochondrial yield is based on measurement

1114   of the concentration of a mitochondrial marker in the tissue homogenate, $C_{mte,thom}$, which

1115   simultaneously provides information on the specific mitochondrial density in the sample (**Fig.**

1116   **8**).

1117   **Table 7. Some useful abbreviations**
1118   **of various sample types, X.**

Identity of sample	X
Mitochondrial preparation	mtprep
Isolated mitochondria	imt
Tissue homogenate	thom
Permeabilized tissue	pti
Permeabilized fibre	pfi
Permeabilized cell	pce
Cell	ce
Organism	org

1119

1120   Tissues can contain multiple cell populations which may have distinct mitochondrial

1121   subtypes. Mitochondria are also in a constant state of flux due to highly dynamic fission and

1122   fusion cycles, and can exist in multiple stages and sizes which may be altered by a range of

1123   factors. The isolation of mitochondria (often achieved through differential centrifugation) can

1124   therefore yield a subsample of the mitochondrial types present in a tissue, dependent on

1125   isolation protocols utilized (*e.g.* centrifugation speed). This possible artefact should be taken

1126   into account when planning experiments using isolated mitochondria. The tendency for

1127   mitochondria of specific sizes to be enriched at different centrifugation speeds also has the

1128   potential to allow the isolation of specific mitochondrial subpopulations and therefore the

1129   analysis of mitochondria from multiple cell lineages within a single tissue.

1130   **Mass-specific flux, J_{mX,O_2}:** Mass-specific flux is obtained by expressing respiration per

1131   mass of sample, m_X [mg]. X is the type of sample, *e.g.*, tissue homogenate, permeabilized fibres

1132   or cells. Volume-specific flux is divided by mass concentration of X, $J_{mX,O_2} = J_{V,O_2}/C_{mX}$; or flow

1133   per cell is divided by mass per cell, $J_{mcell,O_2} = I_{cell,O_2}/M_{cell}$. If mass-specific O_2 flux is constant

1134   and independent of sample size (expressed as mass), then there is no interaction between the

1135   subsystems. A 1.5 mg and a 3.0 mg muscle sample respires at identical mass-specific flux.

1136   Mass-specific O_2 flux, however, may change with the mass of a tissue sample, cells or isolated

1137   mitochondria in the measuring chamber, in which case the nature of the interaction becomes an

1138   issue. Optimization of cell density and arrangement is generally important and particularly in

1139   experiments carried out in wells, considering the confluency of the cell monolayer or clumps

1140   of cells (Salabei *et al.* 2014).

1141   **Number concentration, C_{NX}:** The experimental *number concentration* of sample in the

1142   case of cells or animals, *e.g.*, nematodes is $C_{NX} = N_X/V$ [x·mL^{-1}], where N_X is the number of

1143   cells or organisms in the chamber (**Table 6**).

1144   **Flow per sample entity, I_{X,O_2}:** A special case of normalization is encountered in

1145   respiratory studies with permeabilized (or intact) cells. If respiration is expressed per cell, the

1146 O_2 flow per measurement system is replaced by the O_2 flow per cell, I_{cell,O_2} (**Table 6**). O_2 flow

1147   can be calculated from volume-specific O_2 flux, J_{V,O_2} [nmol·s^{-1}·L^{-1}] (per V of the measurement

1148   chamber [L]), divided by the number concentration of cells, $C_{Nce} = N_{ce}/V$ [cell·L^{-1}], where N_{ce}

1149   is the number of cells in the chamber. Cellular O_2 flow can be compared between cells of

1150   identical size. To take into account changes and differences in cell size, further normalization

1151   is required to obtain cell size-specific or mitochondrial marker-specific O_2 flux (Renner *et al.*

1152   2003).

1153   The complexity changes when the sample is a whole organism studied as an experimental

1154   model. The well-established scaling law in respiratory physiology reveals a strong interaction

1155   of O_2 consumption and individual body mass of an organism, since *basal* metabolic rate (flow)

1156   does not increase linearly with body mass, whereas *maximum* mass-specific O_2 flux, $\dot{V}_{O2max}$ or

1157 $\dot{V}_{O2peak}$, is approximately constant across a large range of individual body mass (Weibel and

1158   Hoppeler 2005), with individuals, breeds, and certain species deviating substantially from this

1159   general relationship. $\dot{V}_{O2peak}$ of human endurance athletes is 60 to 80 mL O_2·min^{-1}·kg^{-1} body

1160   mass, converted to $J_{m,O2peak}$ of 45 to 60 nmol·s^{-1}·g^{-1} (Gnaiger 2014; **Table 8**).

1161

1162   *4.3. Normalization for mitochondrial content*

1163   Normalization is a problematic subject and it is essential to consider the question of the

1164   study. If the study aims to compare tissue performance, such as the effects of a certain treatment

1165   on a specific tissue, then normalization can be successful, using tissue mass or protein content,

1166   for example. If the aim, however, is to find differences of mitochondrial function independent

1167   of mitochondrial density (**Table 6**), then normalization to a mitochondrial marker is imperative

1168   (**Fig. 9**). However, one cannot assume that quantitative changes in various markers such as

1169   mitochondrial proteins necessarily occur in parallel with one another. It is important to first

1170 establish that the marker chosen is not selectively altered by the performed treatment. In

1171 conclusion, the normalization must reflect the question under investigation to reach a satisfying

1172 answer. On the other hand, the goal of comparing results across projects and institutions

1173 requires some standardization on normalization for entry into a databank.

1174   **Mitochondrial concentration, C_{mte}, and mitochondrial markers:** It is important that

1175 mitochondrial concentration in the tissue and the measurement chamber be quantified, as a

1176 physiological output and result of mitochondrial biogenesis and degradation, and as a quantity

1177 for normalization in functional analyses. Mitochondrial organelles comprise a cellular

1178 reticulum that is in a continual flux of fusion and fission. Hence the definition of an "amount"

1179 of mitochondria is often misconceived: mitochondria cannot be counted as a number of

1180 occurring elements. Therefore, quantification of the "amount" of mitochondria depends on

1181 measurement of chosen mitochondrial markers. 'Mitochondria are the structural and functional

1182 elemental units of cell respiration' (Gnaiger 2014). The quantity of a mitochondrial marker can

1183 be considered as the measurement of the amount of *elemental mitochondrial units* or

1184 *mitochondrial elements*, mte. However, since mitochondrial quality changes under certain

1185 stimuli, particularly in mitochondrial dysfunction and after exercise training (Pesta *et al.* 2011;

1186 Campos *et al.* 2017), some markers can vary while other markers are unchanged. (*1*)

1187 Mitochondrial volume and membrane area are structural markers, whereas mitochondrial

1188 protein mass is frequently used as a marker for isolated   mitochondria. (*2*) Molecular and

1189 enzymatic mitochondrial markers (amounts or activities) can be selected as matrix markers,

1190 *e.g.*, citrate synthase activity, mtDNA; mtIM-markers, *e.g.*, cytochrome *c* oxidase activity, aa_3

1191 content, cardiolipin, or mtOM-markers, *e.g.*, TOM20. (*3*) Extending the measurement of

1192 mitochondrial marker enzyme activity to mitochondrial pathway capacity, measured as ET- or

1193 OXPHOS-capacity, can be considered as an integrative functional mitochondrial marker.

1194   Depending on the type of mitochondrial marker, the mitochondrial elements, mte, are

1195 expressed in marker-specific units. Although concentration and density are used synonymously

1196   in physical chemistry, it is recommended to distinguish *experimental mitochondrial*

1197   *concentration*, $C_{mte} = mte/V$ and *physiological mitochondrial density*, $D_{mte} = mte/m_X$. Then

1198   mitochondrial density is the amount of mitochondrial elements per mass of tissue (**Fig. 9**). The

1199   former is mitochondrial density multiplied by sample mass concentration, $C_{mte} = D_{mte} \cdot C_{mX}$, or

1200   mitochondrial content multiplied by sample number concentration, $C_{mte} = mte_X \cdot C_{NX}$ (**Table 6**).

1201

1202

1203   **Fig. 9. Structure-function analysis of performance of an organism, organ or tissue,**

1204   **or a cell (sample entity X). O$_2$ flow, I_{X,O_2}, is the product of performance per functional**

1205   **element (element function, mitochondria-specific flux), element density**

1206   **(mitochondrial density, D_{mte}), and size of entity X (mass M_X).** (**A**) Structured analysis:

1207   performance is the product of mitochondrial *function* (mt-specific flux) and *structure*

1208   (functional elements; D_{mte} times mass of X). (**B**) Unstructured analysis: performance is

1209   the product of *entity mass-specific flux, $J_{mX,O_2} = I_{X,O_2}/M_X = I_{O_2}/m_X$* [mol·s^{-1}·kg^{-1}] and *size of*

1210   *entity*, expressed as mass of X; $M_X = m_X \cdot N_X^{-1}$ [kg·x^{-1}]. See **Table 6** for further explanation

1211   of quantities and units. Modified from Gnaiger (2014).

1212

1213   **Mitochondria-specific flux, J_{mte,O_2}:** Volume-specific metabolic O_2 flux depends on: (*1*)

1214   the sample concentration in the volume of the instrument chamber, C_{mX}, or C_{NX}; (*2*) the

1215   mitochondrial density in the sample, $D_{mte} = mte/m_X$ or $mte_X = mte/N_X$; and (*3*) the specific

1216   mitochondrial activity or performance per elemental mitochondrial unit, $J_{mte,O_2} = J_{V,O_2}/C_{mte}$

1217   (**Table 6**). Obviously, the numerical results for J_{mte,O_2} vary according to the type of

1218   mitochondrial marker chosen for measurement of mte and $C_{mte} = mte/V$.

1219

1220   *4.4. Evaluation of mitochondrial markers*

1221   Different methods are implicated in quantification of mitochondrial markers and have

1222   different strengths. Some problems are common for all mitochondrial markers, mte: (*1*)

1223   Accuracy of measurement is crucial, since even a highly accurate and reproducible

1224   measurement of O_2 flux results in an inaccurate and noisy expression normalized for a biased

1225   and noisy measurement of a mitochondrial marker. This problem is acute in mitochondrial

1226   respiration because the denominators used (the mitochondrial markers) are often very small

1227   moieties whose accurate and precise determination is difficult. This problem can be avoided

1228   when O_2 fluxes measured in substrate-uncoupler-inhibitor titration protocols are normalized for

1229   flux in a defined respiratory reference state, which is used as an *internal* marker and yields flux

1230   control ratios, *FCR*s (**Fig. 7**). *FCR*s are independent of any *externally* measured markers and,

1231   therefore, are statistically very robust, considering the limitations of ratios in general (Jasienski

1232   and Bazzaz 1999). *FCR*s indicate qualitative changes of mitochondrial respiratory control, with

1233   highest quantitative resolution, separating the effect of mitochondrial density or concentration

1234   on J_{mX,O_2} and I_{X,O_2} from that of function per elemental mitochondrial marker, J_{mte,O_2} (Pesta *et al.*

1235   2011; Gnaiger 2014). (*2*) If mitochondrial quality does not change and only the amount of

1236   mitochondria, defined by the chosen mitochondrial marker, varies as a determinant of mass-

1237   specific flux, any marker is equally qualified in principle; then in practice selection of the

1238   optimum marker depends only on the accuracy and precision of measurement of the

1239 mitochondrial marker. (*3*) If mitochondrial flux control ratios change, then there may not be

1240 any best mitochondrial marker. In general, measurement of multiple mitochondrial markers

1241 enables a comparison and evaluation of normalization for a variety of mitochondrial markers.

1242 Particularly during postnatal development, the activity of marker enzymes, such as cytochrome

1243 *c* oxidase and citrate synthase, follows different time courses (Drahota et al. 2004). Evaluation

1244 of mitochondrial markers in healthy controls is insufficient for providing guidelines for

1245 application in the diagnosis of pathological states and specific treatments.

1246   In line with the concept of the respiratory control ratio (Chance and Williams 1955a), the

1247 most readily used normalization is that of flux control ratios and flux control factors (Gnaiger

1248 2014). Selection of the state of maximum flux in a protocol as the reference state has the

1249 advantages of (*1*) internal normalization, (*2*) statistical linearization of the response in the range

1250 of 0 to 1, and (*3*) consideration of maximum flux for integrating a very large number of

1251 elemental steps in the OXPHOS- or ET-pathways. This reduces the risk of selecting a functional

1252 marker that is specifically altered by the treatment or pathodology, yet increases the chance that

1253 the highly integrative pathway is disproportionately affected, *e.g.* the OXPHOS- rather than

1254 ET-pathway in case of an enzymatic defect in the phosphorylation-pathway. In this case,

1255 additional information can be obtained by reporting flux control ratios based on a reference

1256 state which indicates stable tissue-mass specific flux. Stereological determination of

1257 mitochondrial content via two-dimensional transmission electron microscopy can have

1258 limitations due to the dynamics of mitochondrial size (Meinild Lundby *et al.* 2017). Accurate

1259 determination of three-dimensional volume by two-dimensional microscopy can be both time

1260 consuming and statistically challenging (Larsen *et al.* 2012). Using mitochondrial marker

1261 enzymes (citrate synthase activity, Complex I–IV amount or activity) for normalization of flux

1262 is limited in part by the same factors that apply to the use of flux control ratios. Strong

1263 correlations between various mitochondrial markers and citrate synthase activity (Reichmann

1264 et al. 1985; Boushel *et al.* 2007; Mogensen *et al.* 2007) are expected in a specific tissue of

1265 healthy subjects and in disease states not specifically targeting citrate synthase. Citrate synthase

1266 activity is acutely modifiable by exercise (Tonkonogi *et al.* 1997; Leek *et al.* 2001). Evaluation

1267 of mitochondrial markers related to a selected age and sex cohort cannot be extrapolated to

1268 provide recommendations for normalization in respirometric diagnosis of disease, in different

1269 states of development and ageing, different cell types, tissues, and species. mtDNA normalised

1270 to nDNA via qPCR is correlated to functional mitochondrial markers including OXPHOS- and

1271 ET-capacity in some cases (Puntschart *et al.* 1995; Wang *et al.* 1999; Menshikova *et al.* 2006;

1272 Boushel *et al.* 2007), but lack of such correlations have been reported (Menshikova *et al.* 2005;

1273 Schultz and Wiesner 2000; Pesta *et al.* 2011). Several studies indicate a strong correlation

1274 between cardiolipin content and increase in mitochondrial functionality with exercise

1275 (Menshikova *et al.* 2005; Menshikova *et al.* 2007; Larsen *et al.* 2012; Faber *et al.* 2014), but its

1276 use as a general mitochondrial biomarker in disease remains questionable.

1277

1278 *4.5. Conversion: units and normalization*

1279   Many different units have been used to report the rate of oxygen consumption, OCR

1280 (**Table 8**). *SI* base units provide the common reference for introducing the theoretical principles

1281 (**Fig. 7**), and are used with appropriately chosen *SI* prefixes to express numerical data in the

1282 most practical format, with an effort towards unification within specific areas of application

1283 (**Table 9**). For studies of cells, we recommend that respiration be expressed, as far as possible,

1284 as (*1*) O_2 flux normalized for a mitochondrial marker, for separation of the effects of

1285 mitochondrial quality and content on cell respiration (this includes *FCR*s as a normalization for

1286 a functional mitochondrial marker); (*2*) O_2 flux in units of cell volume or mass, for comparison

1287 of respiration of cells with different cell size (Renner *et al.* 2003) and with studies on tissue

1288 preparations, and (*3*) O_2 flow in units of attomole (10^{-18} mol) of O_2 consumed by each cell in a

1289 second [$amol \cdot s^{-1} \cdot cell^{-1}$], numerically equivalent to [$pmol \cdot s^{-1} \cdot 10^{-6}$ cells]. This convention allows

1290 information to be easily used when designing experiments in which oxygen consumption must

1291 be considered. For example, to estimate the volume-specific O_2 flux in an instrument chamber

1292 that would be expected at a particular cell number concentration, one simply needs to multiply

1293 the flow per cell by the number of cells per volume of interest. This provides the amount of O_2

1294 [mol] consumed per time [s^{-1}] per unit volume [L^{-1}]. At an O_2 flow of 100 amol·s^{-1}·cell^{-1} and a

1295 cell density of 10^9 cells·L^{-1} (10^6 cells·mL^{-1}), the volume-specific O_2 flux is 100 nmol·s^{-1}·L^{-1} (100

1296 pmol·s^{-1}·mL^{-1}).

1297   Although volume is expressed as m^3 using the *SI* base unit, the litre [dm^3] is the basic unit

1298 of volume for concentration and is used for most solution chemical kinetics. If one multiplies

1299 I_{cell,O_2} by C_{Ncell}, then the result will not only be the amount of O_2 [mol] consumed per time [s^{-1}]

1300 in one litre [L^{-1}], but also the change in the concentration of oxygen per second (for any volume

1301 of an ideally closed system). This is ideal for kinetic modeling as it blends with chemical rate

1302 equations where concentrations are typically expressed in mol·L^{-1} (Wagner *et al.* 2011). In

1303 studies of multinuclear cells, such as differentiated skeletal muscle cells, it is easy to determine

1304 the number of nuclei but not the total number of cells. A generalized concept, therefore, is

1305 obtained by substituting cells by nuclei as the sample entity. This does not hold, however, for

1306 enucleated platelets.

1307

1308 *4.5. Conversion: oxygen, proton and ATP flux*

1309 $J_{O_2,k}$ is coupled in mitochondrial steady states to proton cycling, $J_{H+\infty} = J_{H+\uparrow} = J_{H+\downarrow}$ (**Fig.**

1310 **2**). $J_{H+\uparrow/n}$ and $J_{H+\downarrow/n}$ [nmol·s^{-1}·L^{-1}] are converted into electrical units, $J_{H+\uparrow/e}$ [mC·s^{-1}·L^{-1} = mA·L^{-1}]

1311 $= J_{H+\uparrow/n}$ [nmol·s^{-1}·L^{-1}]·F [C·mol^{-1}]·10^{-6} (**Table 4**). At a $J_{H+\uparrow}/J_{O_2,k}$ ratio or H$^+\uparrow$/O_2 of 20 (H$^+\uparrow$/O =

1312 10), a volume-specific O_2 flux of 100 nmol·s^{-1}·L^{-1} would correspond to a proton flux of 2,000

1313 nmol H$^+\uparrow$·s^{-1}·L^{-1} or volume-specific current of 193 mA·L^{-1}.

1314 $$J_{V,H+\uparrow/e} \text{ [mA·L}^{-1}] = J_{V,H+\uparrow/n}·F·10^{-6} \text{ [nmol·s}^{-1}·L^{-1}·mC·nmol^{-1}] \qquad \text{(Eq. 5.1)}$$

1315 $$J_{V,H+\uparrow/e} \text{ [mA·L}^{-1}] = J_{V,O_2}·(H^+\uparrow/O_2)·F·10^{-6} \text{ [mC·s}^{-1}·L^{-1} = mA·L^{-1}] \qquad \text{(Eq. 5.2)}$$

1316 ET-capacity in various human cell types including HEK 293, primary HUVEC and fibroblasts

1317 ranges from 50 to 180 $amol \cdot s^{-1} \cdot cell^{-1}$, measured in intact cells in the noncoupled state (see

1318 Gnaiger 2014). At 100 $amol \cdot s^{-1} \cdot cell^{-1}$ corrected for ROX (corresponding to a catabolic power

1319 of -48 $pW \cdot cell^{-1}$), the current across the mt-membranes, I_e, approximates 193 $pA \cdot cell^{-1}$ or 0.2

1320 nA per cell. See Rich (2003) for an extension of quantitative bioenergetics from the molecular

1321 to the human scale, with a transmembrane proton flux equivalent to 520 A in an adult at a

1322 catabolic power of -110 W. Modelling approaches illustrate the link between proton motive

1323 force and currents (Willis *et al.* 2016). For NADH- and succinate-linked respiration, the

1324 mechanistic P»/O_2 ratio (referring to the full 4 electron reduction of O_2) is calculated at 20/3.7

1325 and 12/3.7, respectively (Eq. 6), equal to 5.4 and 3.3. The classical P»/O ratios (referring to the

1326 2 electron reduction of 0.5 O_2) are 2.7 and 1.6 (Watt *et al.* 2010), in direct agreement with the

1327 measured P»/O ratio for succinate of 1.58 ± 0.02 (Gnaiger *et al.* 2000; for detailed reviews see

1328 Wikström and Hummer 2012; Sazanov 2015),

$$P»/O_2 = (H^+\uparrow/O_2)/(H^+\downarrow/P») \qquad \text{(Eq. 6)}$$

1330 In summary (**Fig. 1**),

$$J_{V,P»} \text{ [nmol} \cdot s^{-1} \cdot L^{-1}] = J_{V,O_2} \cdot (H^+\uparrow/O_2)/(H^+\downarrow/P») \qquad \text{(Eq. 7.1)}$$

$$J_{V,P»} \text{ [nmol} \cdot s^{-1} \cdot L^{-1}] = J_{V,O_2} \cdot (P»/O_2) \qquad \text{(Eq. 7.2)}$$

1333 We consider isolated mitochondria as powerhouses and proton pumps as molecular

1334 machines to relate experimental results to energy metabolism of the intact cell. The cellular

1335 P»/O_2 based on oxidation of glycogen is increased by the glycolytic (fermentative) substrate-

1336 level phosphorylation of 3 P»/Glyc, *i.e.*, 0.5 mol P» for each mol O_2 consumed in the complete

1337 oxidation of a mol glycosyl unit (Glyc). Adding 0.5 to the mitochondrial P»/O_2 ratio of 5.4

1338 yields a bioenergetic cell physiological P»/O_2 ratio close to 6. Two NADH equivalents are

1339 formed during glycolysis and transported from the cytosol into the mitochondrial matrix, either

1340 by the malate-aspartate shuttle or by the glycerophosphate shuttle resulting in different

1341 theoretical yield of ATP generated by mitochondria, the energetic cost of which potentially

1342 must be taken into account. Considering also substrate-level phosphorylation in the TCA cycle,

1343 this high P»/O$_2$ ratio not only reflects proton translocation and OXPHOS studied in isolation,

1344 but integrates mitochondrial physiology with energy transformation in the living cell (Gnaiger

1345 1993a).

1346

1347 **Table 8. Conversion of various units used in respirometry and**

1348 **ergometry.** e is the number of electrons or reducing equivalents. z_B is the

1349 charge number of entity B.

1350

1 Unit	x	Multiplication factor	*SI*-Unit	Note
ng.atom O·s^{-1}	(2 e)	0.5	nmol O$_2$·s^{-1}	
ng.atom O·min^{-1}	(2 e)	8.33	pmol O$_2$·s^{-1}	
natom O·min^{-1}	(2 e)	8.33	pmol O$_2$·s^{-1}	
nmol O$_2$·min^{-1}	(4 e)	16.67	pmol O$_2$·s^{-1}	
nmol O$_2$·h^{-1}	(4 e)	0.2778	pmol O$_2$·s^{-1}	
mL O$_2$·min^{-1} at STPD^a		0.744	μmol O$_2$·s^{-1}	1
W = J/s at -470 kJ/mol O$_2$		-2.128	μmol O$_2$·s^{-1}	
mA = mC·s^{-1}	(z_{H^+} = 1)	10.36	nmol H$^+$·s^{-1}	2
mA = mC·s^{-1}	(z_{O_2} = 4)	2.59	nmol O$_2$·s^{-1}	2
nmol H$^+$·s^{-1}	(z_{H^+} = 1)	0.09649	mA	3
nmol O$_2$·s^{-1}	(z_{O_2} = 4)	0.38594	mA	3

1351

1352 1 At standard temperature and pressure dry (STPD: 0 °C = 273.15 K and 1 atm =

1353   101.325 kPa = 760 mmHg), the molar volume of an ideal gas, V_m, and V_{m,O_2} is

1354   22.414 and 22.392 L·mol^{-1} respectively. Rounded to three decimal places, both

1355   values yield the conversion factor of 0.744. For comparison at NTPD (20 °C),

1356 V_{m,O_2} is 24.038 L·mol^{-1}. Note that the *SI* standard pressure is 100 kPa.

1357 2 The multiplication factor is $10^6/(z_B·F)$.

1358 3 The multiplication factor is $z_B·F/10^6$.

Table 9. Conversion of units with preservation of numerical values.

Name	Frequently used unit	Equivalent unit	Note
Volume-specific flux, J_{V,O_2}	$pmol \cdot s^{-1} \cdot mL^{-1}$	$nmol \cdot s^{-1} \cdot L^{-1}$	1
	$mmol \cdot s^{-1} \cdot L^{-1}$	$mol \cdot s^{-1} \cdot m^{-3}$	
Cell-specific flow, I_{O_2}	$pmol \cdot s^{-1} \cdot 10^{-6}$ cells	$amol \cdot s^{-1} \cdot cell^{-1}$	2
	$pmol \cdot s^{-1} \cdot 10^{-9}$ cells	$zmol \cdot s^{-1} \cdot cell^{-1}$	3
Cell number concentration, C_{Nce}	10^6 cells$\cdot mL^{-1}$	10^9 cells$\cdot L^{-1}$	
Mitochondrial protein concentration, C_{mte}	0.1 mg$\cdot mL^{-1}$	0.1 g$\cdot L^{-1}$	
Mass-specific flux, J_{m,O_2}	$pmol \cdot s^{-1} \cdot mg^{-1}$	$nmol \cdot s^{-1} \cdot g^{-1}$	4
Catabolic power, $P_{O_2,k}$	$\mu W \cdot 10^{-6}$ cells	$pW \cdot cell^{-1}$	1
Volume	$1,000$ L	m^3 ($1,000$ kg)	
	L	dm^3 (kg)	
	mL	cm^3 (g)	
	μL	mm^3 (mg)	
	fL	μm^3 (pg)	5
Amount of substance concentration	$M = mol \cdot L^{-1}$	$mol \cdot dm^{-3}$	

1   pmol: picomole $= 10^{-12}$ mol
2   amol: attomole $= 10^{-18}$ mol
3   zmol: zeptomole $= 10^{-21}$ mol
4   nmol: nanomole $= 10^{-9}$ mol
5   1 fL $= 10^{-15}$ L

5. Conclusions

MitoEAGLE can serve as a gateway to better diagnose mitochondrial respiratory defects linked to genetic variation, age-related health risks, sex-specific mitochondrial performance, lifestyle with its effects on degenerative diseases, and thermal and chemical environment. The present recommendations on coupling control states and rates, linked to the concept of the protonmotive force (Part 1) will be extended in a series of reports on pathway control of mitochondrial respiration, respiratory states in intact cells, and harmonization of experimental procedures.

Box 5: Mitochondrial and cell respiration

Mitochondrial and cell respiration is the process of highly exergonic and exothermic energy transformation in which scalar redox reactions are coupled to vectorial ion translocation across

1380 a semipermeable membrane, which separates the small volume of a bacterial cell or

1381 mitochondrion from the larger volume of its surroundings. The electrochemical exergy can be

1382 partially conserved in the phosphorylation of ADP to ATP or in ion pumping, or dissipated in

1383 an electrochemical short-circuit. Respiration is thus clearly distinguished from fermentation as

1384 the counterpart of cellular core energy metabolism. Respiration is separated in mitochondrial

1385 preparations from the partial contribution of fermentative pathways of the intact cell. According

1386 to this definition, residual oxygen consumption, as measured after inhibition of mitochondrial

1387 electron transfer, does not belong to the class of catabolic reactions and is, therefore, subtracted

1388 from total oxygen consumption to obtain baseline-corrected respiration.

1389

1390   The optimal choice for expressing mitochondrial and cell respiration (**Box 5**) as O_2 flow

1391 per biological system, and normalization for specific tissue-markers (volume, mass, protein)

1392 and mitochondrial markers (volume, protein, content, mtDNA, activity of marker enzymes,

1393 respiratory reference state) is guided by the scientific question under study. Interpretation of

1394 the obtained data depends critically on appropriate normalization, and therefore reporting rates

1395 merely as $nmol \cdot s^{-1}$ is discouraged, since it restricts the analysis to intra-experimental

1396 comparison of relative (qualitative) differences. Expressing O_2 consumption per cell may not

1397 be possible when dealing with tissues. For studies with mitochondrial preparations, we

1398 recommend that normalizations be provided as far as possible: (*1*) on a per cell basis as O_2 flow

1399 (a biophysical normalization); (*2*) per g cell or tissue protein, or per cell or tissue mass as mass-

1400 specific O_2 flux (a cellular normalization); and (*3*) per mitochondrial marker as mt-specific flux

1401 (a mitochondrial normalization). With information on cell size and the use of multiple

1402 normalizations, maximum potential information is available (Renner *et al.* 2003; Wagner *et al.*

1403 2011; Gnaiger 2014). When using isolated mitochondria, mitochondrial protein is a frequently

1404 applied mitochondrial marker, the use of which is basically restricted to isolated mitochondria.

1405 Mitochondrial markers, such as citrate synthase activity as an enzymatic matrix marker, provide

1406   a link to the tissue of origin on the basis of calculating the mitochondrial yield, *i.e.*, the fraction

1407   of mitochondrial marker obtained from a unit mass of tissue.

1408

1414

1415   **6. References** (*incomplete; www links will be deleted in the final version*)

1416   Altmann R (1894) Die Elementarorganismen und ihre Beziehungen zu den Zellen. Zweite

1417   vermehrte Auflage. Verlag Von Veit & Comp, Leipzig:160 pp. -

1418   www.mitoeagle.org/index.php/Altmann_1894_Verlag_Von_Veit_%26_Comp

1419   Beard DA (2005) A biophysical model of the mitochondrial respiratory system and oxidative

1420   phosphorylation. PLoS Comput Biol 1(4):e36. -

1421   http://www.mitoeagle.org/index.php/Beard_2005_PLOS_Comput_Biol

1422   Birkedal R, Laasmaa M, Vendelin M (2014) The location of energetic compartments affects

1423   energetic communication in cardiomyocytes. Front Physiol 5:376. doi:

1424   10.3389/fphys.2014.00376. eCollection 2014. PMID: 25324784

1425   Breton S, Beaupré HD, Stewart DT, Hoeh WR, Blier PU (2007) The unusual system of

1426   doubly uniparental inheritance of mtDNA: isn't one enough? Trends Genet 23:465-74.

1427   Brown GC (1992) Control of respiration and ATP synthesis in mammalian mitochondria and

1428   cells. Biochem J 284:1-13. - www.mitoeagle.org/index.php/Brown_1992_Biochem_J

1429   Campos JC, Queliconi BB, Bozi LHM, Bechara LRG, Dourado PMM, Andres AM, Jannig

1430   PR, Gomes KMS, Zambelli VO, Rocha-Resende C, Guatimosim S, Brum PC, Mochly-

1431   Rosen D, Gottlieb RA, Kowaltowski AJ, Ferreira JCB (2017) Exercise reestablishes

1432   autophagic flux and mitochondrial quality control in heart failure. Autophagy 13:1304-

1433   317.

1434   Chance B, Williams GR (1955a) Respiratory enzymes in oxidative phosphorylation. I.

1435   Kinetics of oxygen utilization. J Biol Chem 217:383-93. -

1436   http://www.mitoeagle.org/index.php/Chance_1955_J_Biol_Chem-I

1437   Chance B, Williams GR (1955b) Respiratory enzymes in oxidative phosphorylation: III. The

1438   steady state. J Biol Chem 217:409-27. -

1439   www.mitoeagle.org/index.php/Chance_1955_J_Biol_Chem-III

1440   Chance B, Williams GR (1955c) Respiratory enzymes in oxidative phosphorylation. IV. The

1441   respiratory chain. J Biol Chem 217:429-38. -

1442   www.mitoeagle.org/index.php/Chance_1955_J_Biol_Chem-IV

1443   Chance B, Williams GR (1956) The respiratory chain and oxidative phosphorylation. Adv

1444   Enzymol Relat Subj Biochem 17:65-134. -

1445   www.mitoeagle.org/index.php/Chance_1956_Adv_Enzymol_Relat_Subj_Biochem

1446   Cobb LJ, Lee C, Xiao J, Yen K, Wong RG, Nakamura HK, Mehta HH, Gao Q, Ashur C,

1447   Huffman DM, Wan J, Muzumdar R, Barzilai N, Cohen P (2016) Naturally occurring

1448   mitochondrial-derived peptides are age-dependent regulators of apoptosis, insulin

1449   sensitivity, and inflammatory markers. Aging (Albany NY) 8:796-809.

1450   Cohen ER, Cvitas T, Frey JG, Holmström B, Kuchitsu K, Marquardt R, Mills I, Pavese F,

1451   Quack M, Stohner J, Strauss HL, Takami M, Thor HL (2008) Quantities, units and

1452   smbols in physical chemistry, IUPAC Green Book, 3rd Edition, 2nd Printing, IUPAC &

1453   RSC Publishing, Cambridge. -

1454   www.mitoeagle.org/index.php/Cohen_2008_IUPAC_Green_Book

1455   Cooper H, Hedges LV, Valentine JC, eds (2009) The handbook of research synthesis and

1456   meta-analysis. Russell Sage Foundation.

1457 Coopersmith J (2010) Energy, the subtle concept. The discovery of Feynman's blocks from

1458   Leibnitz to Einstein. Oxford University Press:400 pp.

1459 Cummins J (1998) Mitochondrial DNA in mammalian reproduction. Rev Reprod 3:172–82.

1460 Dai Q, Shah AA, Garde RV, Yonish BA, Zhang L, Medvitz NA, Miller SE, Hansen EL, Dunn

1461   CN, Price TM (2013) A truncated progesterone receptor (PR-M) localizes to the

1462   mitochondrion and controls cellular respiration. Mol Endocrinol 27:741-53.

1463 Divakaruni AS, Brand MD (2011) The regulation and physiology of mitochondrial proton

1464   leak. Physiology (Bethesda) 26:192-205.

1465 Doskey CM, van 't Erve TJ, Wagner BA, Buettner GR (2015) Moles of a substance per cell is

1466   a highly informative dosing metric in cell culture. PLOS ONE 10:e0132572. -

1467   http://dx.doi.org/doi:10.1371/journal.pone.0132572

1468 Drahota Z, Milerová M, Stieglerová A, Houstek J, Ostádal B (2004) Developmental changes

1469   of cytochrome *c* oxidase and citrate synthase in rat heart homogenate. Physiol Res

1470   53:119-22.

1471 Duarte FV, Palmeira CM, Rolo AP (2014) The role of microRNAs in mitochondria: small

1472   players acting wide. Genes (Basel) 5:865-86.

1473 Dufour S, Rousse N, Canioni P, Diolez P (1996) Top-down control analysis of temperature

1474   effect on oxidative phosphorylation. Biochem J 314:743-51.

1475 Ernster L, Schatz G (1981) Mitochondria: a historical review. J Cell Biol 91:227s-55s. -

1476   www.mitoeagle.org/index.php/Ernster_1981_J_Cell_Biol

1477 Estabrook RW (1967) Mitochondrial respiratory control and the polarographic measurement

1478   of ADP:O ratios. Methods Enzymol 10:41-7. -

1479   www.mitoeagle.org/index.php/Estabrook_1967_Methods_Enzymol

1480 Faber C, Zhu ZJ, Castellino S, Wagner DS, Brown RH, Peterson RA, Gates L, Barton J,

1481   Bickett M, Hagerty L, Kimbrough C, Sola M, Bailey D, Jordan H, Elangbam CS (2014)

1482   Cardiolipin profiles as a potential biomarker of mitochondrial health in diet-induced

1483   obese mice subjected to exercise, diet-restriction and ephedrine treatment. J Appl

1484   Toxicol 34:1122-9.

1485   Fell D (1997) Understanding the control of metabolism. Portland Press.

1486   Garlid KD, Beavis AD, Ratkje SK (1989) On the nature of ion leaks in energy-transducing

1487   membranes. Biochim Biophys Acta 976:109-20. -

1488   www.mitoeagle.org/index.php/Garlid_1989_Biochim_Biophys_Acta

1489   Garlid KD, Semrad C, Zinchenko V. Does redox slip contribute significantly to mitochondrial

1490   respiration? In: Schuster S, Rigoulet M, Ouhabi R, Mazat J-P, eds (1993) Modern trends

1491   in biothermokinetics. Plenum Press, New York, London:287-93.

1492   Gerö D, Szabo C (2016) Glucocorticoids suppress mitochondrial oxidant production via

1493   upregulation of uncoupling protein 2 in hyperglycemic endothelial cells. PLoS One

1494   11:e0154813.

1495   Gibney E (2017) New definitions of scientific units are on the horizon. Nature 550:312–13. -

1496   https://www.nature.com/news/new-definitions-of-scientific-units-are-on-the-horizon-

1497   1.22837

1498   Gnaiger E. Efficiency and power strategies under hypoxia. Is low efficiency at high glycolytic

1499   ATP production a paradox? In: Surviving Hypoxia: Mechanisms of Control and

1500   Adaptation. Hochachka PW, Lutz PL, Sick T, Rosenthal M, Van den Thillart G, eds

1501   (1993a) CRC Press, Boca Raton, Ann Arbor, London, Tokyo:77-109. -

1502   www.mitoeagle.org/index.php/Gnaiger_1993_Hypoxia

1503   Gnaiger E (1993b) Nonequilibrium thermodynamics of energy transformations. Pure Appl

1504   Chem 65:1983-2002. - www.mitoeagle.org/index.php/Gnaiger_1993_Pure_Appl_Chem

1505   Gnaiger E (2001) Bioenergetics at low oxygen: dependence of respiration and

1506   phosphorylation on oxygen and adenosine diphosphate supply. Respir Physiol 128:277-

1507   97. - www.mitoeagle.org/index.php/Gnaiger_2001_Respir_Physiol

1508 Gnaiger E (2009) Capacity of oxidative phosphorylation in human skeletal muscle. New

1509   perspectives of mitochondrial physiology. Int J Biochem Cell Biol 41:1837-45. -

1510   www.mitoeagle.org/index.php/Gnaiger_2009_Int_J_Biochem_Cell_Biol

1511 Gnaiger E (2014) Mitochondrial pathways and respiratory control. An introduction to

1512   OXPHOS analysis. 4th ed. Mitochondr Physiol Network 19.12. Oroboros MiPNet

1513   Publications, Innsbruck:80 pp. -

1514   www.mitoeagle.org/index.php/Gnaiger_2014_MitoPathways

1515 Gnaiger E, Méndez G, Hand SC (2000) High phosphorylation efficiency and depression of

1516   uncoupled respiration in mitochondria under hypoxia. Proc Natl Acad Sci USA

1517   97:11080-5. -

1518   www.mitoeagle.org/index.php/Gnaiger_2000_Proc_Natl_Acad_Sci_U_S_A

1519 Greggio C, Jha P, Kulkarni SS, Lagarrigue S, Broskey NT, Boutant M, Wang X, Conde

1520   Alonso S, Ofori E, Auwerx J, Cantó C, Amati F (2017) Enhanced respiratory chain

1521   supercomplex formation in response to exercise in human skeletal muscle. Cell Metab

1522   25:301-11. - http://www.mitoeagle.org/index.php/Greggio_2017_Cell_Metab

1523 Hofstadter DR (1979) Gödel, Escher, Bach: An eternal golden braid. A metaphorical fugue on

1524   minds and machines in the spirit of Lewis Carroll. Harvester Press:499 pp. -

1525   www.mitoeagle.org/index.php/Hofstadter_1979_Harvester_Press

1526 Illaste A, Laasmaa M, Peterson P, Vendelin M (2012) Analysis of molecular movement

1527   reveals latticelike obstructions to diffusion in heart muscle cells. Biophys J 102:739-48.

1528   - PMID: 22385844

1529 Jasienski M, Bazzaz FA (1999) The fallacy of ratios and the testability of models in biology.

1530   Oikos 84:321-26.

1531 Jepihhina N, Beraud N, Sepp M, Birkedal R, Vendelin M (2011) Permeabilized rat

1532   cardiomyocyte response demonstrates intracellular origin of diffusion obstacles.

1533   Biophys J 101:2112-21. - PMID: 22067148

1534 Klepinin A, Ounpuu L, Guzun R, Chekulayev V, Timohhina N, Tepp K, Shevchuk I,

1535   Schlattner U, Kaambre T (2016) Simple oxygraphic analysis for the presence of

1536   adenylate kinase 1 and 2 in normal and tumor cells. J Bioenerg Biomembr 48:531-48. -

1537   http://www.mitoeagle.org/index.php/Klepinin_2016_J_Bioenerg_Biomembr

1538 Klingenberg M (2017) UCP1 - A sophisticated energy valve. Biochimie 134:19-27.

1539 Koit A, Shevchuk I, Ounpuu L, Klepinin A, Chekulayev V, Timohhina N, Tepp K, Puurand

1540   M,Truu L, Heck K, Valvere V, Guzun R, Kaambre T (2017) Mitochondrial respiration

1541   in human colorectal and breast cancer clinical material is regulated differently. Oxid

1542   Med Cell Longev 1372640. -

1543   http://www.mitoeagle.org/index.php/Koit_2017_Oxid_Med_Cell_Longev

1544 Komlódi T, Tretter L (2017) Methylene blue stimulates substrate-level phosphorylation

1545   catalysed by succinyl-CoA ligase in the citric acid cycle. Neuropharmacology 123:287-

1546   98. - www.mitoeagle.org/index.php/Komlodi_2017_Neuropharmacology

1547 Lane N (2005) Power, sex, suicide: Mitochondria and the meaning of life. Oxford University

1548   Press:354 pp.

1549 Larsen S, Nielsen J, Neigaard Nielsen C, Nielsen LB, Wibrand F, Stride N, Schroder HD,

1550   Boushel RC, Helge JW, Dela F, Hey-Mogensen M (2012) Biomarkers of mitochondrial

1551   content in skeletal muscle of healthy young human subjects. J Physiol 590:3349-60. -

1552   http://www.mitoeagle.org/index.php/Larsen_2012_J_Physiol

1553 Lee C, Zeng J, Drew BG, Sallam T, Martin-Montalvo A, Wan J, Kim SJ, Mehta H, Hevener

1554   AL, de Cabo R, Cohen P (2015) The mitochondrial-derived peptide MOTS-c promotes

1555   metabolic homeostasis and reduces obesity and insulin resistance. Cell Metab 21:443-

1556   54.

1557 Lee SR, Kim HK, Song IS, Youm J, Dizon LA, Jeong SH, Ko TH, Heo HJ, Ko KS, Rhee BD,

1558   Kim N, Han J (2013) Glucocorticoids and their receptors: insights into specific roles in

1559   mitochondria. Prog Biophys Mol Biol 112:44-54.

1560 Leek BT, Mudaliar SR, Henry R, Mathieu-Costello O, Richardson RS (2001) Effect of acute

1561   exercise on citrate synthase activity in untrained and trained human skeletal muscle. Am

1562   J Physiol Regul Integr Comp Physiol 280:R441-7.

1563 Lemieux H, Blier PU, Gnaiger E (2017) Remodeling pathway control of mitochondrial

1564   respiratory capacity by temperature in mouse heart: electron flow through the Q-

1565   junction in permeabilized fibers. Sci Rep 7:2840. -

1566   www.mitoeagle.org/index.php/Lemieux_2017_Sci_Rep

1567 Lenaz G, Tioli G, Falasca AI, Genova ML (2017) Respiratory supercomplexes in

1568   mitochondria. In: Mechanisms of primary energy trasduction in biology. M Wikstrom

1569   (ed) Royal Society of Chemistry Publishing, London, UK:296-337.

1570 Margulis L (1970) Origin of eukaryotic cells. New Haven: Yale University Press.

1571 Meinild Lundby AK, Jacobs RA, Gehrig S, de Leur J, Hauser M, Bonne TC, Flück D,

1572   Dandanell S, Kirk N, Kaech A, Ziegler U, Larsen S, Lundby C (2017) Exercise training

1573   increases skeletal muscle mitochondrial volume density by enlargement of existing

1574   mitochondria and not de novo biogenesis. Acta Physiol (Oxf) [Epub ahead of print].

1575 Menshikova EV, Ritov VB, Fairfull L, Ferrell RE, Kelley DE, Goodpaster BH (2006) Effects

1576   of exercise on mitochondrial content and function in aging human skeletal muscle. J

1577   Gerontol A Biol Sci Med Sci 61:534-40.

1578 Menshikova EV, Ritov VB, Ferrell RE, Azuma K, Goodpaster BH, Kelley DE (2007)

1579   Characteristics of skeletal muscle mitochondrial biogenesis induced by moderate-

1580   intensity exercise and weight loss in obesity. J Appl Physiol (1985) 103:21-7.

1581 Menshikova EV, Ritov VB, Toledo FG, Ferrell RE, Goodpaster BH, Kelley DE (2005)

1582   Effects of weight loss and physical activity on skeletal muscle mitochondrial function in

1583   obesity. Am J Physiol Endocrinol Metab 288:E818-25.

1584 Miller GA (1991) The science of words. Scientific American Library New York:276 pp. -

1585   www.mitoeagle.org/index.php/Miller_1991_Scientific_American_Library

1586 Mitchell P (1961) Coupling of phosphorylation to electron and hydrogen transfer by a chemi-

1587 osmotic type of mechanism. Nature 191:144-8. -

1588 http://www.mitoglobal.org/index.php/Mitchell_1961_Nature

1589 Mitchell P (2011) Chemiosmotic coupling in oxidative and photosynthetic phosphorylation.

1590 Biochim Biophys Acta Bioenergetics 1807:1507-38. -

1591 http://www.sciencedirect.com/science/article/pii/S0005272811002283

1592 Mitchell P, Moyle J (1967) Respiration-driven proton translocation in rat liver mitochondria.

1593 Biochem J 105:1147-62. - www.mitoeagle.org/index.php/Mitchell_1967_Biochem_J

1594 Mogensen M, Sahlin K, Fernström M, Glintborg D, Vind BF, Beck-Nielsen H, Højlund K

1595 (2007) Mitochondrial respiration is decreased in skeletal muscle of patients with type 2

1596 diabetes. Diabetes 56:1592-9.

1597 Moreno M, Giacco A, Di Munno C, Goglia F (2017) Direct and rapid effects of 3,5-diiodo-L-

1598 thyronine (T2). Mol Cell Endocrinol 7207:30092-8.

1599 Morrow RM, Picard M, Derbeneva O, Leipzig J, McManus MJ, Gouspillou G, Barbat-Artigas

1600 S, Dos Santos C, Hepple RT, Murdock DG, Wallace DC (2017) Mitochondrial energy

1601 deficiency leads to hyperproliferation of skeletal muscle mitochondria and enhanced

1602 insulin sensitivity. Proc Natl Acad Sci U S A 114:2705-10. -

1603 www.mitoeagle.org/index.php/Morrow_2017_Proc_Natl_Acad_Sci_U_S_A

1604 Nicholls DG, Ferguson S (2013) Bioenergetics 4. Elsevier.

1605 Paradies G, Paradies V, De Benedictis V, Ruggiero FM, Petrosillo G (2014) Functional role

1606 of cardiolipin in mitochondrial bioenergetics. Biochim Biophys Acta 1837:408-17. -

1607 http://www.mitoeagle.org/index.php/Paradies_2014_Biochim_Biophys_Acta

1608 Pesta D, Hoppel F, Macek C, Messner H, Faulhaber M, Kobel C, Parson W, Burtscher M,

1609 Schocke M, Gnaiger E (2011) Similar qualitative and quantitative changes of

1610 mitochondrial respiration following strength and endurance training in normoxia and

1611 hypoxia in sedentary humans. Am J Physiol Regul Integr Comp Physiol 301:R1078–87.

1612   Price TM, Dai Q (2015) The role of a mitochondrial progesterone receptor (PR-M) in

1613   progesterone action. Semin Reprod Med 33:185-94.

1614   Prigogine I (1967) Introduction to thermodynamics of irreversible processes. Interscience,

1615   New York, 3rd ed:147pp.

1616   Puchowicz MA, Varnes ME, Cohen BH, Friedman NR, Kerr DS, Hoppel CL (2004)

1617   Oxidative phosphorylation analysis: assessing the integrated functional activity of

1618   human skeletal muscle mitochondria – case studies. Mitochondrion 4:377-85. -

1619   www.mitoeagle.org/index.php/Puchowicz_2004_Mitochondrion

1620   Puntschart A, Claassen H, Jostarndt K, Hoppeler H, Billeter R (1995) mRNAs of enzymes

1621   involved in energy metabolism and mtDNA are increased in endurance-trained athletes.

1622   Am J Physiol 269:C619-25.

1623   Quiros PM, Mottis A, Auwerx J (2016) Mitonuclear communication in homeostasis and

1624   stress. Nat Rev Mol Cell Biol 17:213-26.

1625   Reichmann H, Hoppeler H, Mathieu-Costello O, von Bergen F, Pette D (1985) Biochemical

1626   and ultrastructural changes of skeletal muscle mitochondria after chronic electrical

1627   stimulation in rabbits. Pflugers Arch 404:1-9.

1628   Renner K, Amberger A, Konwalinka G, Gnaiger E (2003) Changes of mitochondrial

1629   respiration, mitochondrial content and cell size after induction of apoptosis in leukemia

1630   cells. Biochim Biophys Acta 1642:115-23. -

1631   www.mitoeagle.org/index.php/Renner_2003_Biochim_Biophys_Acta

1632   Rich P (2003) Chemiosmotic coupling: The cost of living. Nature 421:583. -

1633   www.mitoeagle.org/index.php/Rich_2003_Nature

1634   Rostovtseva TK, Sheldon KL, Hassanzadeh E, Monge C, Saks V, Bezrukov SM, Sackett DL

1635   (2008) Tubulin binding blocks mitochondrial voltage-dependent anion channel and

1636   regulates respiration. Proc Natl Acad Sci USA 105:18746-51. -

1637   www.mitoeagle.org/index.php/Rostovtseva_2008_Proc_Natl_Acad_Sci_U_S_A

1638   Rustin P, Parfait B, Chretien D, Bourgeron T, Djouadi F, Bastin J, Rötig A, Munnich A

1639   (1996) Fluxes of nicotinamide adenine dinucleotides through mitochondrial membranes

1640   in human cultured cells. J Biol Chem 271:14785-90.

1641   Saks VA, Veksler VI, Kuznetsov AV, Kay L, Sikk P, Tiivel T, Tranqui L, Olivares J, Winkler

1642   K, Wiedemann F, Kunz WS (1998) Permeabilised cell and skinned fiber techniques in

1643   studies of mitochondrial function in vivo. Mol Cell Biochem 184:81-100. -

1644   http://www.mitoeagle.org/index.php/Saks_1998_Mol_Cell_Biochem

1645   Salabei JK, Gibb AA, Hill BG (2014) Comprehensive measurement of respiratory activity in

1646   permeabilized cells using extracellular flux analysis. Nat Protoc 9:421-38.

1647   Sazanov LA (2015) A giant molecular proton pump: structure and mechanism of respiratory

1648   complex I. Nat Rev Mol Cell Biol 16:375-88. -

1649   www.mitoeagle.org/index.php/Sazanov_2015_Nat_Rev_Mol_Cell_Biol

1650   Schneider TD (2006) Claude Shannon: biologist. The founder of information theory used

1651   biology to formulate the channel capacity. IEEE Eng Med Biol Mag 25:30-3.

1652   Schönfeld P, Dymkowska D, Wojtczak L (2009) Acyl-CoA-induced generation of reactive

1653   oxygen species in mitochondrial preparations is due to the presence of peroxisomes.

1654   Free Radic Biol Med 47:503-9.

1655   Schrödinger E (1944) What is life? The physical aspect of the living cell. Cambridge Univ

1656   Press. - www.mitoeagle.org/index.php/Gnaiger_1994_BTK

1657   Schultz J, Wiesner RJ (2000) Proliferation of mitochondria in chronically stimulated rabbit

1658   skeletal muscle--transcription of mitochondrial genes and copy number of

1659   mitochondrial DNA. J Bioenerg Biomembr 32:627-34.

1660   Simson P, Jepihhina N, Laasmaa M, Peterson P, Birkedal R, Vendelin M (2016) Restricted

1661   ADP movement in cardiomyocytes: Cytosolic diffusion obstacles are complemented

1662   with a small number of open mitochondrial voltage-dependent anion channels. J Mol

1663   Cell Cardiol 97:197-203. - PMID: 27261153

1664   Stucki JW, Ineichen EA (1974) Energy dissipation by calcium recycling and the efficiency of

1665   calcium transport in rat-liver mitochondria. Eur J Biochem 48:365-75.

1666   Tonkonogi M, Harris B, Sahlin K (1997) Increased activity of citrate synthase in human

1667   skeletal muscle after a single bout of prolonged exercise. Acta Physiol Scand 161:435-

1668   6.

1669   Waczulikova I, Habodaszova D, Cagalinec M, Ferko M, Ulicna O, Mateasik A, Sikurova L,

1670   Ziegelhöffer A (2007) Mitochondrial membrane fluidity, potential, and calcium

1671   transients in the myocardium from acute diabetic rats. Can J Physiol Pharmacol 85:372-

1672   81.

1673   Wagner BA, Venkataraman S, Buettner GR (2011) The rate of oxygen utilization by cells.

1674   Free Radic Biol Med 51:700-712. -

1675   http://dx.doi.org/10.1016/j.freeradbiomed.2011.05.024 PMCID: PMC3147247

1676   Wang H, Hiatt WR, Barstow TJ, Brass EP (1999) Relationships between muscle

1677   mitochondrial DNA content, mitochondrial enzyme activity and oxidative capacity in

1678   man: alterations with disease. Eur J Appl Physiol Occup Physiol 80:22-7.

1679   Wang T (2010) Coulomb force as an entropic force. Phys Rev D 81:104045. -

1680   www.mitoeagle.org/index.php/Wang_2010_Phys_Rev_D

1681   Watt IN, Montgomery MG, Runswick MJ, Leslie AG, Walker JE (2010) Bioenergetic cost of

1682   making an adenosine triphosphate molecule in animal mitochondria. Proc Natl Acad Sci

1683   U S A 107:16823-7. -

1684   www.mitoeagle.org/index.php/Watt_2010_Proc_Natl_Acad_Sci_U_S_A

1685   Weibel ER, Hoppeler H (2005) Exercise-induced maximal metabolic rate scales with muscle

1686   aerobic capacity. J Exp Biol 208:1635–44.

1687   White DJ, Wolff JN, Pierson M, Gemmell NJ (2008) Revealing the hidden complexities of

1688   mtDNA inheritance. Mol Ecol 17:4925–42.

1689   Wikström M, Hummer G (2012) Stoichiometry of proton translocation by respiratory

1690   complex I and its mechanistic implications. Proc Natl Acad Sci U S A 109:4431-6. -

1691   www.mitoeagle.org/index.php/Wikstroem_2012_Proc_Natl_Acad_Sci_U_S_A

1692   Willis WT, Jackman MR, Messer JI, Kuzmiak-Glancy S, Glancy B (2016) A simple hydraulic

1693   analog model of oxidative phosphorylation. Med Sci Sports Exerc 48:990-1000.